Opioidergic modulation of inhibitory synaptic transmission in the rat insular cortex

Eiko Yokota
Nihon University Graduate School of Dentistry
Major in Anesthesiology
(Directors: Profs. Yoshiyuki Oi and Masayuki Kobayashi,
and Assis. Prof. Yuko Koyanagi)

Index

This thesis is based on the following two articles:

1) Opioid subtype- and cell type-dependent regulation of inhibitory synaptic transmission in the rat insular cortex.
   Eiko Yokota, Yuko Koyanagi, Kiyofumi Yamamoto, Yoshiyuki Oi, Noriaki Koshikawa, Masayuki Kobayashi. Neuroscience 339:478-490, 2016
2) Opposite effects of mu and delta opioid receptor agonists on excitatory propagation induced in rat somatosensory and insular cortices by dental pulp stimulation.
   Eiko Yokota, Yuko Koyanagi, Hiroko Nakamura, Eri Horinuki, Yoshiyuki Oi, Masayuki Kobayashi. Neurosci Lett 628:52-58, 2016

Abstract

The insular cortex (IC) plays a key role in the cortical modulation of pain processing. The IC neurons express opioid receptors including mu (MOR), kappa (KOR), and delta (DOR) subtypes. Although the suppressive effect of opioidergic agonists on cortical excitatory synaptic transmission has been addressed, little is known about opioidergic roles in inhibitory synaptic transmission, which critically regulates excitatory propagation in the cerebral cortex. The present study aimed to examine the effects of opioid receptor agonists on unitary inhibitory postsynaptic currents (uIPSCs) and on cortical excitatory propagation in the IC.

Multiple whole-cell patch-clamp recordings from rat IC pyramidal and GABAergic neurons were performed. [D-Ala^2,N-Me-Phe^4,Gly^5-ol]-Enkephalin acetate salt (DAMGO), an MOR agonist, reduced uIPSC amplitude by 74% in fast-spiking GABAergic interneuron (FS)→FS connections without a significant effect on FS→pyramidal cell (Pyr) connections. These effects of DAMGO were also observed in non-FS→FS and non-FS→Pyr connections: DAMGO reduced the uIPSC amplitude in non-FS→FS but not in non-FS→Pyr connections. DAMGO-induced depression of uIPSCs was blocked by the MOR antagonist, D-Phe-Cys-Tyr-D-Trp-Arg-Thr-Pen-Thr-NH_2. The DOR agonist, [D-Pen^{2,5}]-Enkephalin hydrate (DPDPE), reduced uIPSC amplitude by 39% in FS→FS and by 49% in FS→Pyr connections, which was antagonized by the DOR antagonist, naltrindole. However, DPDPE had little effect on non-FS→FS/Pyr connections. (±)-trans-U-50488 methanesulfonate salt (U50488), a KOR agonist, had little effect on uIPSC in FS→FS/Pyr connections.

In vivo optical imaging was performed to evaluate the opioidergic effects on cortical excitatory propagation responding to electrical stimulation of dental pulps. To assess the opioidergic effects on the cortical circuits, the electrical stimulation to the maxillary 1st molar pulp was applied, which induced excitation in the ventral part of the primary (S1) and the secondary somatosensory (S2) areas/insular oral region (IOR). The initial excitatory response was observed 10-14 ms after stimulation, and then excitation propagated concentrically. DAMGO suppressed the amplitude of cortical excitation and shrank the maximum excitation areas in S1 and S2/IOR. In contrast, DPDPE increased the amplitude of excitation and expanded the area of maximum excitation. U50488 had little effect on cortical excitation.

These results suggest that MOR-induced uIPSC suppression in FS/non-FS→FS, but not FS/non-FS→Pyr connections, results in the suppression of excitatory propagation in the IC, which may be an underlying mechanism of the powerful analgesic effects of MOR agonists.

CHAPTER I

Opioid subtype- and cell-type-dependent regulation of inhibitory synaptic transmission in the rat insular cortex

Introduction

Pain is an unpleasant experience comprising both somatosensory and emotional components. Somatosensory information of nociception is largely processed in the primary and secondary somatosensory cortex (lateral system), whereas emotional information is likely to be mediated by the insular (IC), anterior cingulate (ACC), orbital, and infralimbic cortices (medial system; Treede et al., 2000). The IC, especially its rostral agranular region (AI), plays a principal role in the cortical modulation of nociceptive information processing (Burkey et al., 1996, 1999; Jasmin et al., 2003; Coffeen et al., 2008, 2011). Jasmin et al. (2004) show that the rostral AI neurons receive nociception inputs from the sensory thalamic nuclei and project to pain-related regions in the brainstem: the dorsal raphe nucleus, periaqueductal gray, and the parabrachial nucleus. These projections from the IC are thought to modulate descending pain inhibition, although the modulation patterns, facilitation or inhibition, remain unresolved (Jasmin et al., 2003). In addition to the nociceptive information from the thalamic nuclei, the IC receives dense projections from the limbic system including the amygdala and cingulate cortex (Krettek and Price, 1977; Allen et al., 1991). Therefore, the rostral AI is thought to integrate the nociception and limbic information during pain processing and to contribute to the descending pain-modulatory control.

Opioids including fentanyl and morphine are the most effective pain killers (Akil et al., 1998; Kieffer and Gavériaux-Ruff, 2002). Opioid receptors are classified into three subtypes—mu (MOR), delta (DOR), and kappa (KOR) (reviewed by McDonald and Lambert, 2013)—all of which couple to the pertussis toxin-sensitive inhibitory G-protein. Activation of these opioid receptors modulates several ion channels in the following manners: (1) the inhibition of voltage-sensitive calcium channels (VSCCs), resulting in suppressed synaptic transmission (McDonald and Lambert, 2005, 2013); (2) the activation of G-protein inwardly rectifying potassium channels; and (3) the decrement of hyperpolarization-activated current, Ih, by the reduction of cAMP (McDonald and Lambert, 2005; Zollner and Stein, 2007). The IC neurons express all subtypes of opioid receptors (Mansour et al., 1988; Svingos et al., 1995; Burkey et al., 1996), and MOR is a principal target of analgesics (Akil et al., 1998; Kieffer and Gavériaux-Ruff, 2002). In fact, Burkey et al. (1996) demonstrated that the microinjection of morphine into the IC reduces neural firing of nociresponsive dorsal horn induced by noxious thermal stimuli, though the mechanisms of MOR-induced modulation of

synaptic transmission have been unknown. In addition, it remains controversial whether MOR's effects on synaptic transmission result in the facilitation or inhibition of excitatory output from the IC. The other opioid receptor subtypes, DOR and KOR, also regulate pain; however, their actions of pain suppression are neither as robust nor as consistent as those of MOR.

Similar to other sensory cortices, the IC local circuit involves several types of inhibitory neurons, i.e., fast-spiking (FS), low-threshold spike, and late-spiking neurons (Koyanagi et al., 2010, 2014; Yamamoto et al., 2010; Kobayashi et al., 2012). Suppressive effects of MOR or DOR agonists have been reported on glutamatergic excitatory synaptic transmission in the ACC pyramidal neurons (Pyr; Tanaka and North, 1994; Zheng, 2010). In contrast, a recent study demonstrates the opposing action of MOR and DOR on excitatory propagation in the IC and adjacent somatosensory cortex in response to the dental pulp stimulation (see Chapter II). These findings suggest the different effects of MOR and DOR on inhibitory synaptic transmission. Although the amplitude of inhibitory postsynaptic potentials (IPSPs) in the ACC pyramidal cells are reduced by a DOR agonist (Tanaka and North, 1994), little information is available regarding GABAergic inhibitory synaptic transmission in the cortex including the IC. A lack of information about the opioidergic modulation of inhibitory synaptic transmission makes the cortical mechanisms of opioidergic pain suppression unclear.

In paired whole-cell patch-clamp recording, pre- and postsynaptic neuron subtypes can be identified, which make precise estimation of opioidergic effects possible. Therefore, paired whole-cell patch-clamp recordings from Pyr and GABAergic interneurons in the rat IC were performed to test the hypothesis that opioid receptor subtypes differentially modulate synaptic transmission depending on pre- and postsynaptic cell types and opioid receptor subtypes.

Materials and Methods

The Institutional Animal Care and Use Committee at Nihon University approved the study protocol, and all experiments were performed according to the National Institutes of Health Guide for the Care and Use of Laboratory Animals. The number of animals used was minimized as well as their suffering.

Brain slice preparations

The techniques for slice preparation and maintenance were almost same as those described previously (Koyanagi et al., 2014; Yamamoto et al., 2015). Briefly, vesicular GABA transporter (VGAT)-Venus line A transgenic rats (Uematsu et al., 2008) of either sex (postnatal days 18-35) were deeply anesthetized with isoflurane (5%). After decapitation, tissue blocks were rapidly removed and submerged in ice-cold modified artificial cerebrospinal fluid (ACSF) (in mM: 230 sucrose, 2.5 KCl, 10 $MgSO_4$, 1.25 NaH_2PO_4, 26 $NaHCO_3$, 2.5 $CaCl_2$, and 10 D-glucose) for 3 min. Coronal slices (350 μm thickness) were

made using a microslicer (Linearslicer Pro 7, Dosaka EM, Kyoto, Japan). The Cortical slices were then incubated at 32°C for 40 min in a submersion-type holding chamber that contained 50% modified ACSF and 50% normal ACSF: (in mM: 126 NaCl, 3 KCl, 2 $MgSO_4$, 1.25 NaH_2PO_4, 26 $NaHCO_3$, 2.0 $CaCl_2$, and 10 D-glucose). All ACSF were aerated with 95% O_2 and 5% CO_2 continuously. Cortical slices were placed in normal ACSF (32°C) for 1 hr and thereafter keeped at room temperature until used for recording.

Whole-cell patch-clamp recording

The slices were transferred to a recording chamber perfused with normal ACSF (2.0 ml/min), and multi whole-cell patch-clamp recordings were performed from Venus-positive fluorescent GABAergic interneurons and Venus-negative Pyr in IC layer V using a fluorescence microscope with Nomarski optics (x 40, ECLIPSE FN1, Nikon, Tokyo, Japan) and an infrared-sensitive video camera (IR-1000, DAGE-MTI, Michigan City, IN, USA). The distance between recorded neurons was < 100 μm. Membrane currents were recorded using amplifiers (Multiclamp 700B, Molecular Devices, Sunnyvale, CA, USA), and digitized (Digidata 1440A, Molecular Devices), observed online, and stored on a computer hard disk using Clampex (pClamp 10, Molecular Devices).

The composition of the internal solution in the pipettes was (in mM) as follows: 70 potassium gluconate, 70 KCl, 10 N-(2-hydroxyethyl)piperazine-N'-(2-ethanesulfonic acid) (HEPES), 2 $MgCl_2$, 2 magnesium adenosine triphosphate (ATP), 0.3 sodium guanosine triphosphate (GTP), and 0.5 EGTA. The internal solution had a pH of 7.3 and an osmolarity of 300 mOsm. The liquid junction potentials were -9 mV, and in this study, the voltage was not corrected. A Flaming-Brown micropipette puller (P-97, Sutter Instruments, Novato, CA, USA) was used to make borosilicate patch electrodes (2-5 MΩ; OD = 1.5 mm, ID = 1.17 mm, Harvard Apparatus, Cambridge, UK).

The recording temperature was set at 30 ± 1 °C. The seal resistance was > 5 GΩ, and the data obtained from electrodes with access resistance of 6-20 MΩ and < 20% change during recordings was included. Before the unitary inhibitory postsynaptic current (uIPSC) recordings, pre- and postsynaptic cell subtypes were identified by neural responses to the application of long (300 ms) hyperpolarizing and depolarizing current pulse injections. Some cell pairs had mutual or ≥ 2 connections, and therefore uIPSC recordings were performed under voltage-clamp conditions (holding potential = -60 mV). To induce action currents in the presynaptic cells, short depolarizing voltage step pulses (2 ms, 80 mV) were applied. [D-Ala^2,N-Me-Phe^4,Gly^5-ol]-Enkephalin acetate salt (DAMGO; Sigma-Aldrich, St. Louis, MO, USA), [D-Pen^{2,5}]-Enkephalin hydrate (DPDPE; Sigma-Aldrich), (±)-trans-U-50488 methanesulfonate salt (U50488; Sigma-Aldrich), D-Phe-Cys-Tyr-D-Trp-Arg-Thr-Pen-Thr-NH_2 (CTAP, Sigma-Aldrich), and naltrindole hydrochloride (naltrindole; Sigma-Aldrich) were dissolved in the perfusate, a normal ACSF. The membrane currents and potentials were low-pass filtered at 5-10 kHz and digitized at 20 kHz.

Data analysis

Clampfit (pClamp 10, Molecular Devices) was used to analyze the firing properties and uIPSC kinetics. The uIPSC whose amplitude was in the range of synaptic noise was regarded to be failure. The uIPSC amplitude, paired-pulse ratio of the 2nd to 1st uIPSC amplitude (PPR), 20-80% rise time, 80-20% decay time, and decay time constant were measured from single uIPSC averaged traces of FS→FS/Pyr connections obtained from 10-20 consecutive traces. Because uIPSC traces in non-FS→FS/Pyr connections showed a wide variation with low signal-to-noise ratio, the rise and decay kinetics of their uIPSCs were inconsistent. Therefore, in non-FS→FS/Pyr connections, the uIPSC amplitude and PPR were only described. PPR was obtained from the averaged uIPSC traces. The failure rate was calculated from 10-20 consecutive sweeps.

Statistics

The data are presented as the mean ± SEM (standard error of the mean). The numbers of cell pairs and animals are presented as *n* and N, respectively. Paired *t*-tests were used to compare the uIPSC kinetics between the control and drug application. Comparisons of the amplitude of uIPSCs between FS→FS and non-FS→FS and between FS→Pyr and non-FS→Pyr connections were performed using Student's *t*-test. Failure rate of uIPSCs between control and drug application was not normally distributed, and therefore, Wilcoxon signed-rank test was used for comparison of failure rate. $P < 0.05$ was considered significant.

Results

A multiple whole-cell patch-clamp technique was used to record uIPSCs from Venus-positive GABAergic and Venus-negative Pyr in layer V of the IC. Venus-positive neurons in the IC were classified into FS and non-FS (Koyanagi et al., 2010, 2014; Yamamoto et al., 2010; Kobayashi et al., 2012). FS is characterized by repetitive firing at high frequencies that frequently exceeds 100 Hz, without adaptation (Fig. 1A), and occupy about half of the GABAergic interneurons in the IC. In addition, the connection rate of FS to Pyr is much higher than that of other GABAergic interneurons, and FS neurons evoke larger amplitudes of IPSCs; therefore, FS neurons were considered as representative inhibitory neurons. In this study, the effects of opioid receptor agonists on uIPSCs obtained from FS→FS and FS→Pyr connections were examined principally. In addition, opioidergic effects on non-FS→FS/Pyr connections were examined, though their uIPSC amplitude was much smaller and connection rate was lower than those of FS→FS/Pyr connections. The present study did not include the cases where postsynaptic cells were non-FS because of their low connection rate from FS.

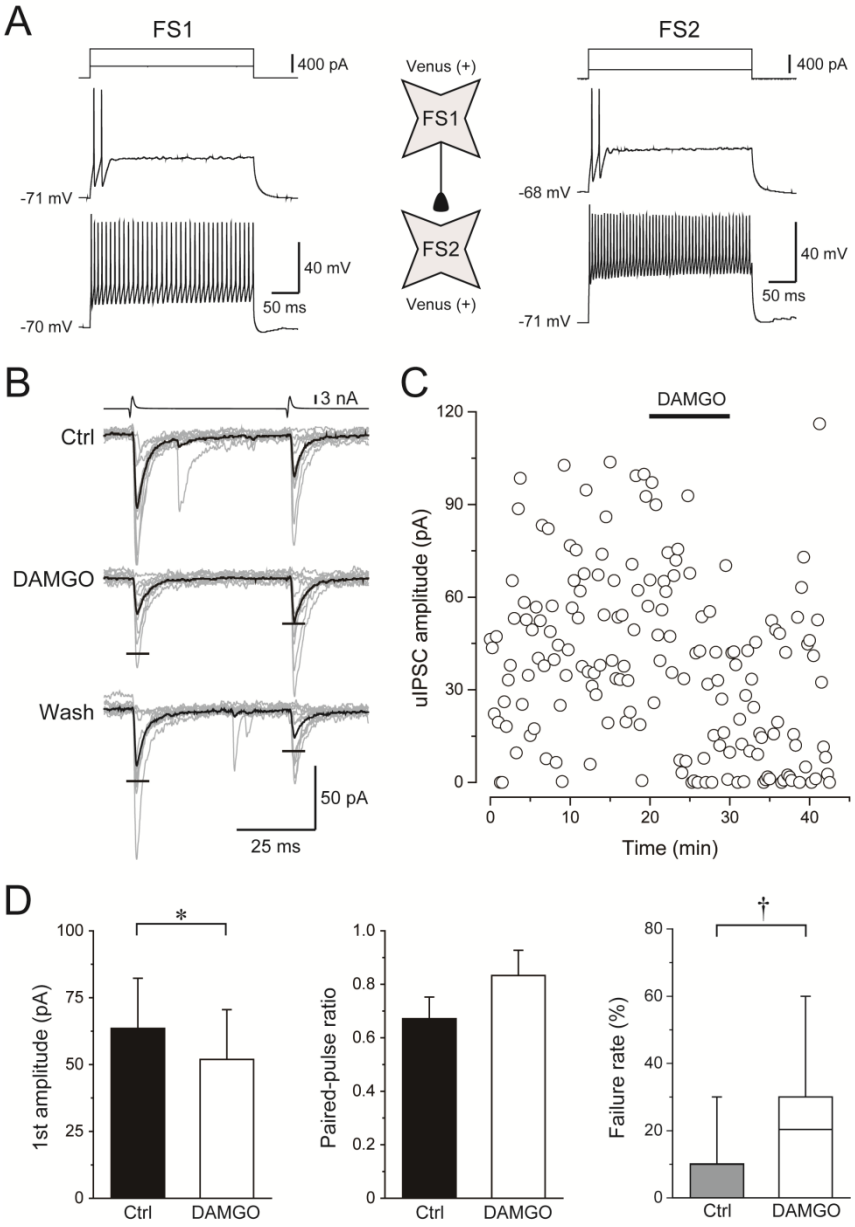

Fig. 1. Inhibitory effects of DAMGO on uIPSCs obtained from FS→FS connections. A: Dual whole-cell patch-clamp recording from two FS in layer V IC. Repetitive firing responses induced by a depolarizing current pulse injection (300 ms) are shown. FS exhibited highly frequent repetitive firing without adaptation. B: uIPSC recordings from postsynaptic FS responding to injection of paired pulses to presynaptic FS (20 Hz, top trace) before (Ctrl), during (DAMGO), and after (Wash) DAMGO (1 μM) application. Ten consecutive traces (grey) and their average traces (black) are shown. Horizontal bars indicate the baseline amplitude. Note that FS showed a depressive effect of DAMGO on uIPSCs. C: Time course of a DAMGO-induced decrease in the 1st uIPSC amplitude recorded from the same pairs as in B. D: First uIPSC amplitude (left), PPR (middle), and failure rate of 1st uIPSCs (right) at baseline and during DAMGO application. Failure rate was represented by a box-and-whisker plot. The ends of the whiskers represent 5% and 95% percentiles. Note depression of the 1st uIPSC amplitude with increasing failure rate by DAMGO. *: $P < 0.05$, paired t-test. †: $P < 0.05$, Wilcoxon test.

Differential effects of MOR on uIPSCs between FS→FS/Pyr connections

First, the effect of DAMGO, an agonist of MOR, was examined which is considered to be a target of pain suppressor (Akil et al., 1998; Kieffer and Gavériaux-Ruff, 2002). A typical example is shown in Fig. 1A-C. Bath application of 1 μM DAMGO effectively reduced the uIPSC amplitude (Fig. 1B,C). The depression of uIPSCs by DAMGO accompanied increases in PPR and failure rate (Fig. 1D). In FS→FS connections, DAMGO consistently reduced the uIPSC amplitude from 63.6 ± 18.7 pA down to 51.9 ± 18.6 pA (73.8 ± 8.3%; $n = 13$; $P < 0.05$,

paired *t*-test; Fig. 1D left). DAMGO-induced reduction of the uIPSC amplitude in FS→FS connections accompanied an increase in the failure rate (9.2 ± 2.6% to 20.8 ± 5.6%, $n = 13$; $P < 0.05$, Wilcoxon signed-rank test; Fig. 1D right), suggesting that the facilitation of uIPSCs by DAMGO is mediated by presynaptic mechanisms. DAMGO tended to increase PPR, although the change was not significant (0.67 ± 0.08 to 0.83 ± 0.09, $n = 13$; $P = 0.14$, paired *t*-test; Fig. 1D middle). DAMGO did not significantly changed PPR (0.67 ± 0.08 to 0.83 ± 0.09, $n = 13$; $P = 0.14$, paired *t*-test; Fig. 1D middle). Moreover, little changes in uIPSC kinetics, including 20-80% rise time (0.4 ± 0.0 ms to 0.4 ± 0.0 ms, $n = 12$; $P = 0.30$, paired *t*-test), 80-20% decay time (4.7 ± 0.4 ms to 4.6 ± 0.4 ms, $n = 12$; $P = 0.58$, paired *t*-test), and decay time constant (5.9 ± 1.3 ms to 4.3 ± 0.8 ms, $n = 12$; $P = 0.33$, paired *t*-test) were observed by application of DAMGO, supporting the above idea of DAMGO's presynaptic modulatory effects.

DAMGO-induced depression of uIPSCs in FS→FS connections was blocked by CTAP (1 μM), a selective MOR antagonist, as shown in Fig. 2. The amplitude of uIPSCs under application of 1 μM CTAP (66.4 ± 10.3 pA) was not significantly changed by 1 μM DAMGO in combination with 1 μM CTAP (70.6 ± 16.2 pA; 100.5 ± 6.6%, $n = 8$, $P = 0.56$, paired-*t* test; Fig. 2C).

In contrast to FS→FS connections, FS→Pyr connections showed no significant DAMGO-induced changes in uIPSC amplitude (107.1 ± 30.1 pA to 118.8 ± 39.4 pA, $n = 16$; $P = 0.39$, paired *t*-test), PPR (0.67 ± 0.05 to 0.92 ± 0.10, $n = 16$; $P = 0.09$, paired *t*-test), or failure rate (8.1 ± 3.8% to 12.5 ± 5.4%, $n = 16$; $P = 0.34$, Wilcoxon signed-rank test; Fig. 3). Therefore, the uIPSC in FS→FS/Pyr showed that the MOR agonist differentially modulates GABA release depending on postsynaptic cell types.

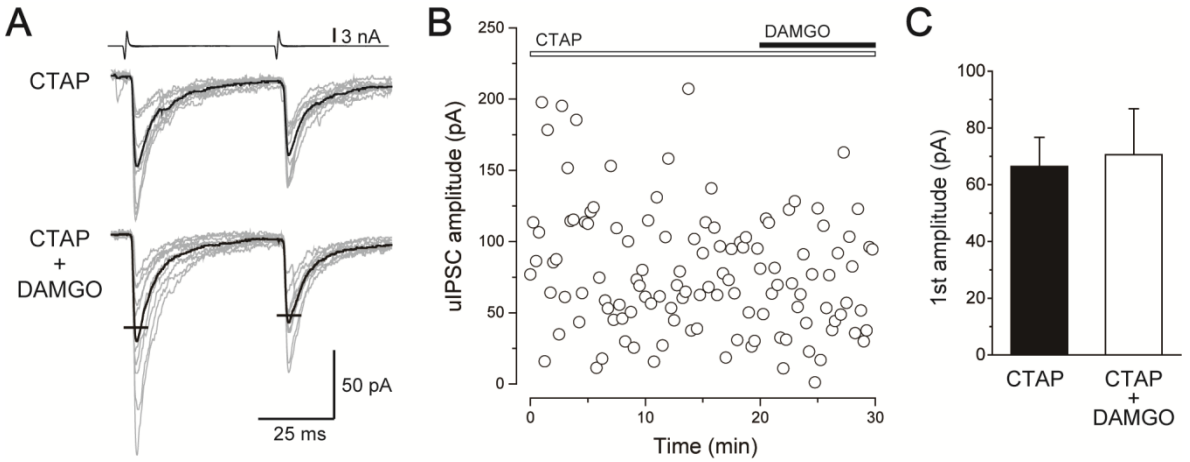

Fig. 2. Effects of DAMGO on uIPSCs obtained from FS→FS connections under application of CTAP (1 μM). A: uIPSC recordings from postsynaptic FS responding to injection of paired pulses to presynaptic FS (20 Hz, top trace) before (CTAP) and during (CTAP + DAMGO) DAMGO application under CTAP application. Ten consecutive traces (grey) and their average traces (black) are shown. Horizontal bars indicate the control amplitude. B: Time course of the 1st uIPSC amplitude recorded from the same pairs as in A. C: First uIPSC amplitude in CTAP and DAMGO with CTAP application. Note that DAMGO had little effect on the amplitude of uIPSCs under application of CTAP.

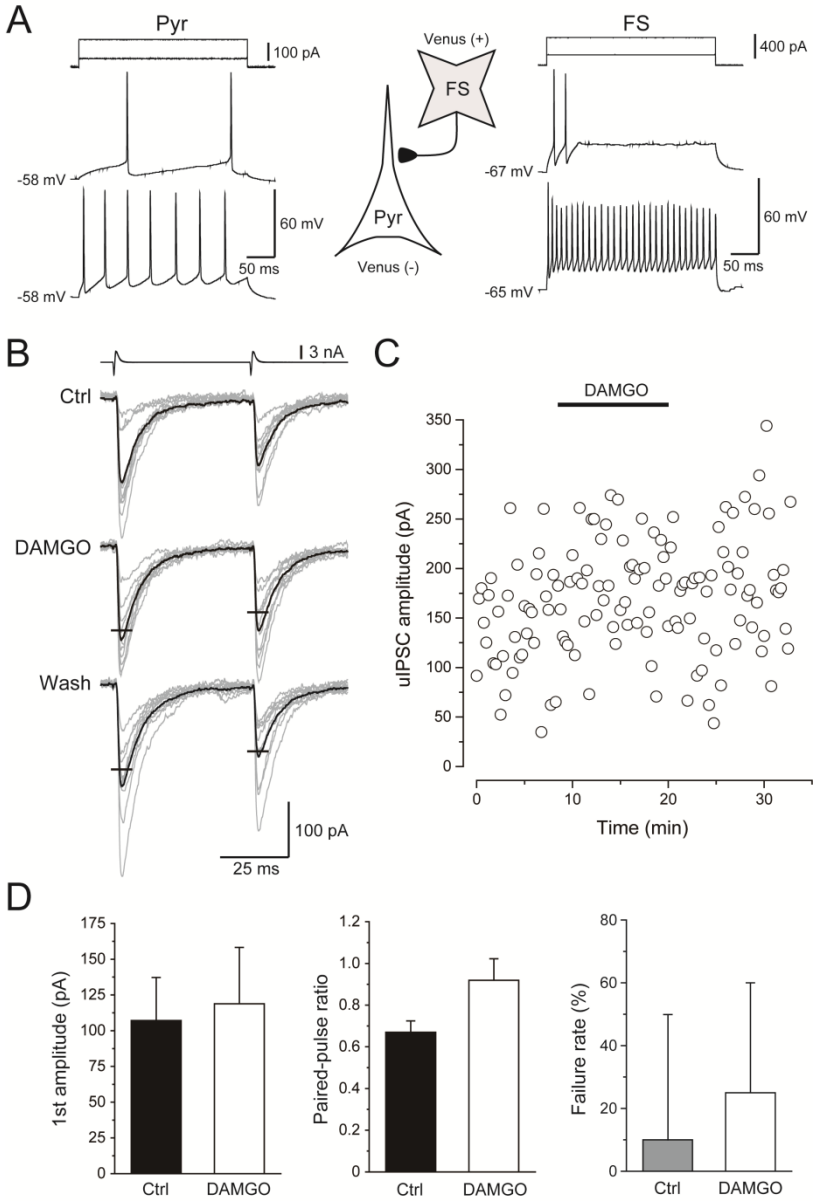

Fig. 3. Small effect of DAMGO on uIPSCs obtained from FS→Pyr connections. A: Dual whole-cell patch-clamp recording from FS and Pyr in layer V IC. Repetitive firing responses induced by depolarizing current pulse injection are shown. Pyr exhibited regular spike firing with adaptation. B: uIPSC recordings from Pyr responding to injection of paired pulses to FS (20 Hz, top trace) before (Ctrl) during (DAMGO), and after (Wash) DAMGO (1 μM) application. Ten consecutive traces (grey) and their average traces (black) are shown. Horizontal bars indicate the baseline amplitude. Note that Pyr showed little effect of DAMGO on uIPSCs. C: Time course of the 1st uIPSC amplitude recorded from the same pairs as in B. D: First uIPSC amplitude (left), PPR (middle), and failure rate of 1st uIPSCs (right) in control and during DAMGO application. Failure rate was represented by a box-and-whisker plot. Note that DAMGO did not significantly change the 1st uIPSC amplitude, PPR, or failure rate.

Similar effects of DAMGO on non-FS→FS and non-FS→Pyr connections

Next, the effects of DAMGO on the uIPSC amplitude of non-FS→FS/Pyr connections were examined. Non-FS→Pyr connections showed much smaller uIPSC amplitude (13.0 ± 3.7 pA, n = 21) in comparison to FS→Pyr connections (89.4 ± 16.4 pA, n = 31, $P < 0.001$, Student's t-test). This tendency was also applicable to the cases that the postsynaptic neuron was FS cells: the uIPSC amplitude of non-FS→FS connections (13.8 ± 3.1 pA, n = 13) was significantly smaller than that of FS→FS connections (89.5 ± 27.8 pA, n = 25, $P < 0.05$, Student's t-test).

Application of 1 μM DAMGO effectively reduced the uIPSC amplitude of non-FS→FS connections from 11.8 ± 3.5 pA to 2.7 ± 0.5 pA (n = 7; P < 0.05, paired t-test; Fig. 4A,B,E). The depression of uIPSCs by DAMGO accompanied an increase in the failure rate (11.4 ± 8.3% to 70.0 ± 7.6%, n = 7; P < 0.05, Wilcoxon signed-rank test; Fig. 4E right), but PPR was not significantly changed (0.67 ± 0.13 to 1.04 ± 0.25, n = 7; P = 0.22, paired t-test; Fig. 4E middle). On the other hand, non-FS→Pyr connections showed an insignificant change in the uIPSC amplitude, though uIPSCs tended to be decreased (12.4 ± 3.2 pA to 6.4 ± 1.3 pA, n = 12; P = 0.12, paired t-test; Fig. 4C-E).

The present findings of DAMGO obtained from FS/non-FS→FS/Pyr connections suggest that the MOR agonist depresses GABA release both from FS and non-FS depending on postsynaptic cell types.

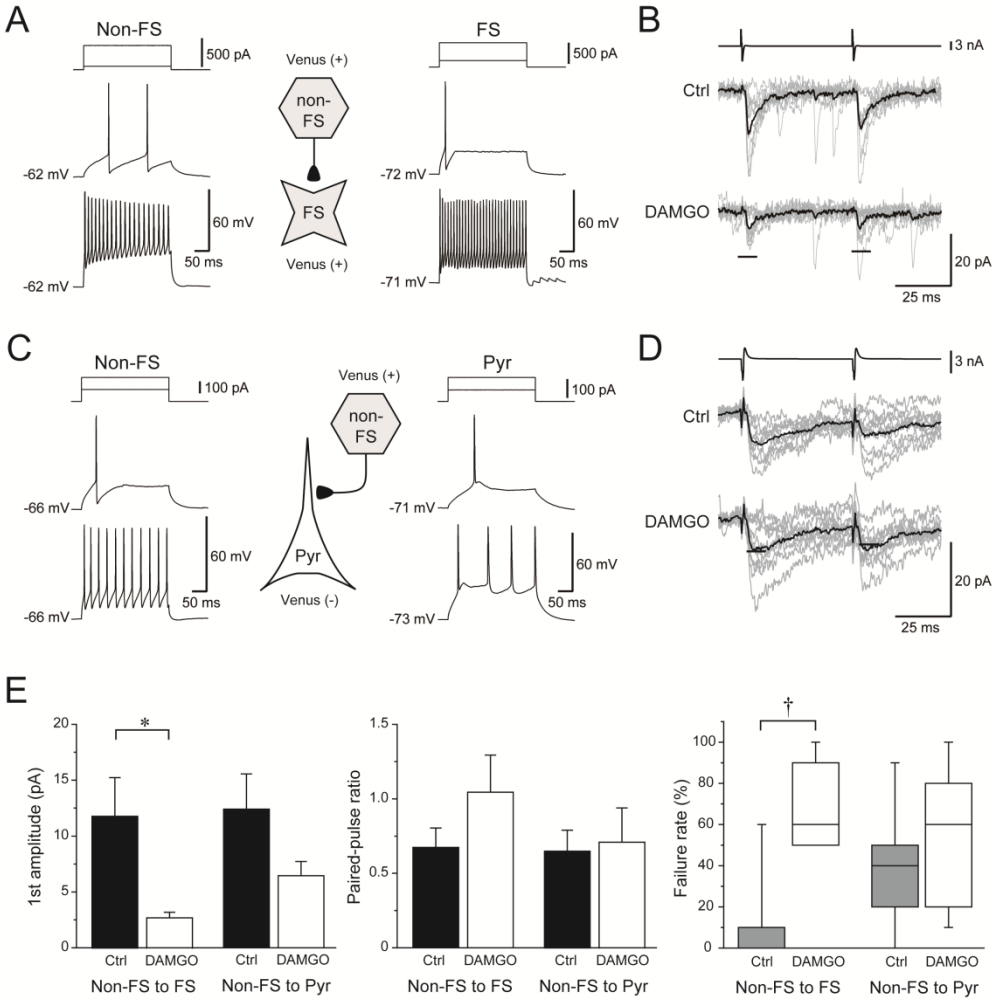

Fig. 4. Effects of DAMGO on uIPSCs obtained from non-FS→FS and non-FS→Pyr connections. A: Dual whole-cell patch-clamp recording from non-FS and FS in layer V IC. Repetitive firing responses induced by depolarizing current pulse injection are shown. Non-FS exhibited regular spike firing with adaptation. B: uIPSC recordings from FS responding to injection of paired pulses to FS (20 Hz, top trace) before (Ctrl) and during DAMGO (1 μM) application. Note that DAMGO depressed uIPSCs. C: Recording from non-FS and Pyr in layer V IC. D: uIPSC recordings from Pyr before (Ctrl) and during DAMGO (1 μM) application. Note that DAMGO had little effect on uIPSCs. E: First uIPSC amplitude (left), PPR (middle), and failure rate of 1st uIPSCs (right) in control and during DAMGO application. Failure rate was represented by a box-and-whisker plot. Note the significant decrease in the 1st uIPSC amplitude and the increase in failure rate by DAMGO in non-FS→FS connections but not in non-FS→Pyr connections. *: P < 0.05, paired t-test. †: P < 0.05, Wilcoxon test.

DOR-induced depression of uIPSCs in FS→FS/Pyr connections

The roles of DOR in uIPSCs were examined by use of DPDPE (1 μM), a DOR agonist, as shown in Figs. 5 and 6. Fig. 5A,B shows a typical example of the effect of DPDPE on uIPSCs in FS→FS connections. Bath application of DPDPE (1 μM) reduced the amplitude of uIPSCs in FS cells, and these suppressive effects were partially recovered. In 12 total FS→FS connections, DPDPE significantly reduced uIPSC amplitude from 117.7 ± 54.5 pA to 47.2 ± 23.3 pA (39.2 ± 5.2%; $P < 0.05$, paired *t*-test; Fig. 5C left). DPDPE significantly increased PPR (0.68 ± 0.08 to 0.99 ± 0.14, $n = 8$; $P < 0.05$, paired *t*-test; Fig. 5C middle) and failure rate (20.0 ± 5.1% to 45.0 ± 9.8%, $n = 12$; $P < 0.01$, Wilcoxon signed-rank test; Fig. 5C right). However, no significant changes in uIPSC kinetics, including 20-80% rise time (0.6 ± 0.1 ms to 0.6 ± 0.1 ms, $n = 9$; $P = 0.45$, paired *t*-test), 80-20% decay time (7.7 ± 1.3 ms to 7.4 ± 1.8 ms, $n = 9$; $P = 0.71$, paired *t*-test), and decay time constant (9.1 ± 1.7 ms to 8.2 ± 2.8 ms, $n = 12$; $P = 0.69$, paired *t*-test) were observed due to application of DPDPE, supporting the above notion of presynaptic modulation by DPDPE.

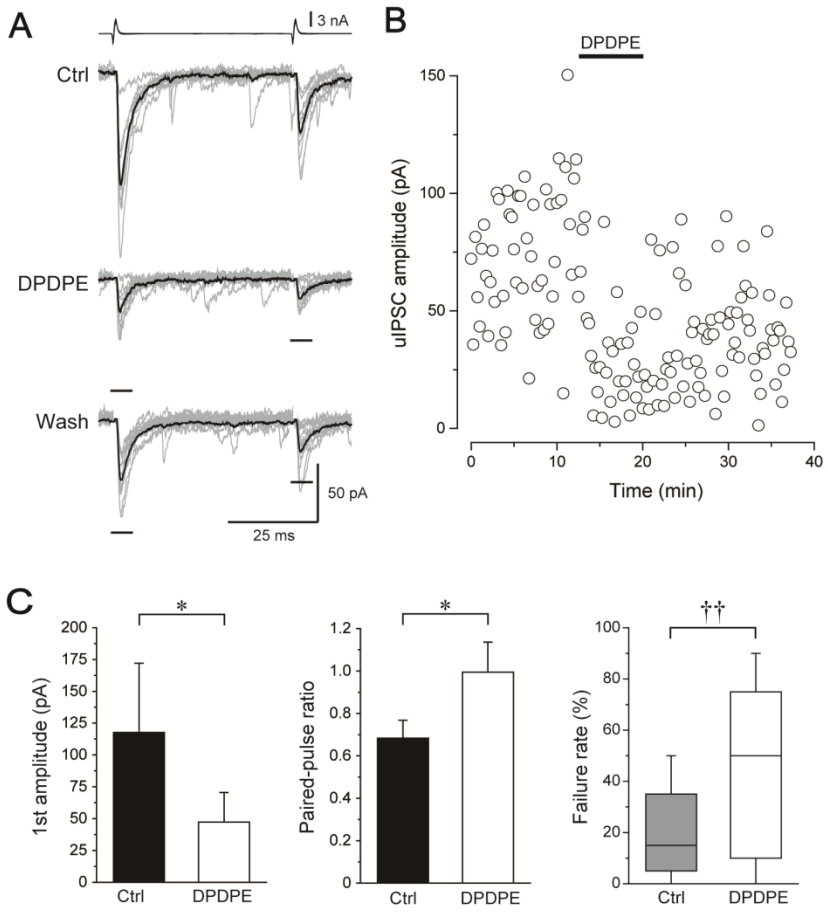

Fig. 5. Inhibitory effects of DPDPE on uIPSCs obtained from FS→FS connections. A: uIPSC recordings from postsynaptic FS responding to injection of paired pulses to presynaptic FS (20 Hz, top trace) before (Ctrl), during (DPDPE), and after (Wash) DPDPE (1 μM) application. Ten consecutive traces (grey) and their average traces (black) are shown. Horizontal bars indicate baseline amplitude. Note that FS had a suppressive effect of DPDPE on uIPSCs. B: Time course of a DPDPE-induced decrease in the 1st uIPSC amplitude recorded from the same pairs as in A. C: First uIPSC amplitude (left), PPR (middle), and failure rate of 1st uIPSCs (right) in control and during DPDPE application. Failure rate was represented by a box-and-whisker plot. Note depression of 1st uIPSC amplitude with increasing failure rate by DPDPE. *: $P < 0.05$, paired *t*-test. ††: $P < 0.01$, Wilcoxon test.

Similar to FS→FS connections, DPDPE reduced the uIPSC amplitude in FS→Pyr connections (70.5 ± 10.7 pA to 32.8 ± 5.4 pA; 49.0 ± 5.6%, n = 15; P < 0.001, paired t-test; Fig. 6). Although PPR showed no significant change by DPDPE (0.87 ± 0.08 to 0.66 ± 0.07, n = 13; P = 0.08, paired t-test; Fig. 6C middle), DPDPE significantly increased the failure rate (8.0 ± 4.6% to 28.0 ± 7.1%, n = 15; P < 0.01, Wilcoxon signed-rank test; Fig. 6C right). Little change in uIPSC kinetics, including 20-80% rise time (0.8 ± 0.1 ms to 0.9 ± 0.1 ms, n = 15; P = 0.38, paired t-test), 80-20% decay time (18.9 ± 1.1 ms to 17.9 ± 2.2 ms, n = 15; P = 0.57, paired t-test), and decay time constant (13.2 ± 1.1 ms to 13.1 ± 1.9 ms, n = 14; P = 0.91, paired t-test), were observed as a result of DPDPE application, again supporting the above idea of the involvement of presynaptic modulation by DPDPE.

The DPDPE-induced suppression of uIPSCs was blocked by naltrindole, a selective DOR antagonist as shown in Fig. 7. The amplitude of uIPSCs did not significantly change as a result of 1 μM DPDPE under application of 1 μM naltrindole in FS→FS connections (55.8 ± 22.9 pA to 58.3 ± 21.5 pA; 120.2 ± 13.2%, n = 11, P = 0.51, paired t-test, Fig. 7C) or in FS→Pyr connections (49.8 ± 16.7 pA to 51.5 ± 17.0 pA; 115.0 ± 12.8%, n = 8, P = 0.70, paired t-test, Fig. 7F).

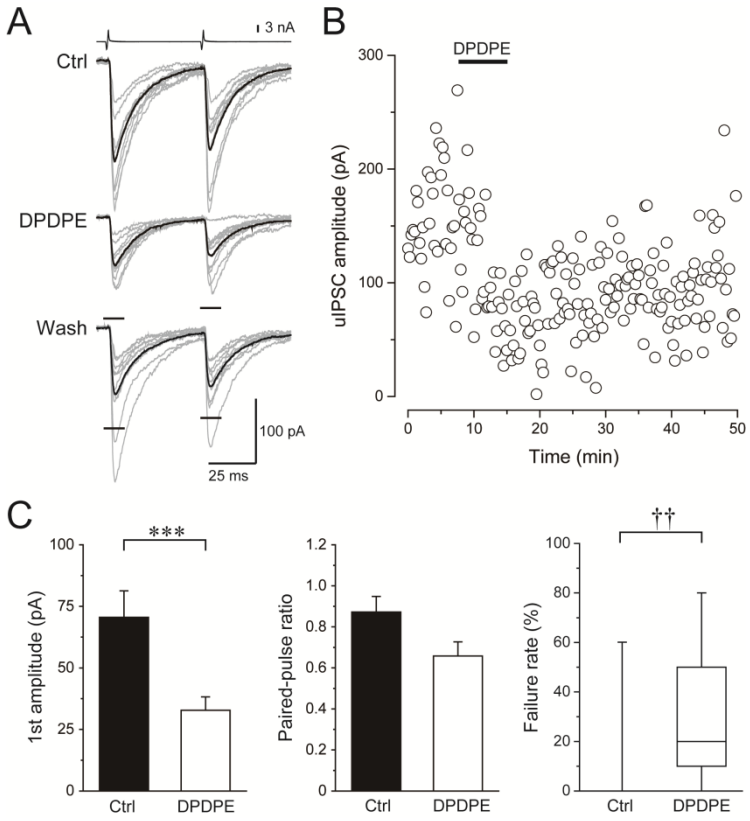

Fig. 6. Inhibitory effects of DPDPE on uIPSCs obtained from FS→Pyr connections. A: uIPSC recordings from Pyr responding to the injection of paired pulses to FS (20 Hz, top trace) before (Ctrl), during (DPDPE), and after (Wash) DPDPE (1 μM) application. Ten consecutive traces (grey) and their average traces (black) are shown. Horizontal bars indicate the amplitude in control. Note that Pyr had a suppressive effect of DPDPE on uIPSCs. B: Time course of DPDPE-induced decrease in the 1st uIPSC amplitude recorded from the same pairs as in A. C: First uIPSC amplitude (left), PPR (middle), and failure rate of 1st uIPSCs (right) in control and during DPDPE application. Failure rate was represented by a box-and-whisker plot. Note depression of the 1st uIPSC amplitude with increasing failure rate by DPDPE. ***: P < 0.001, paired t-test. ††: P < 0.01, Wilcoxon test.

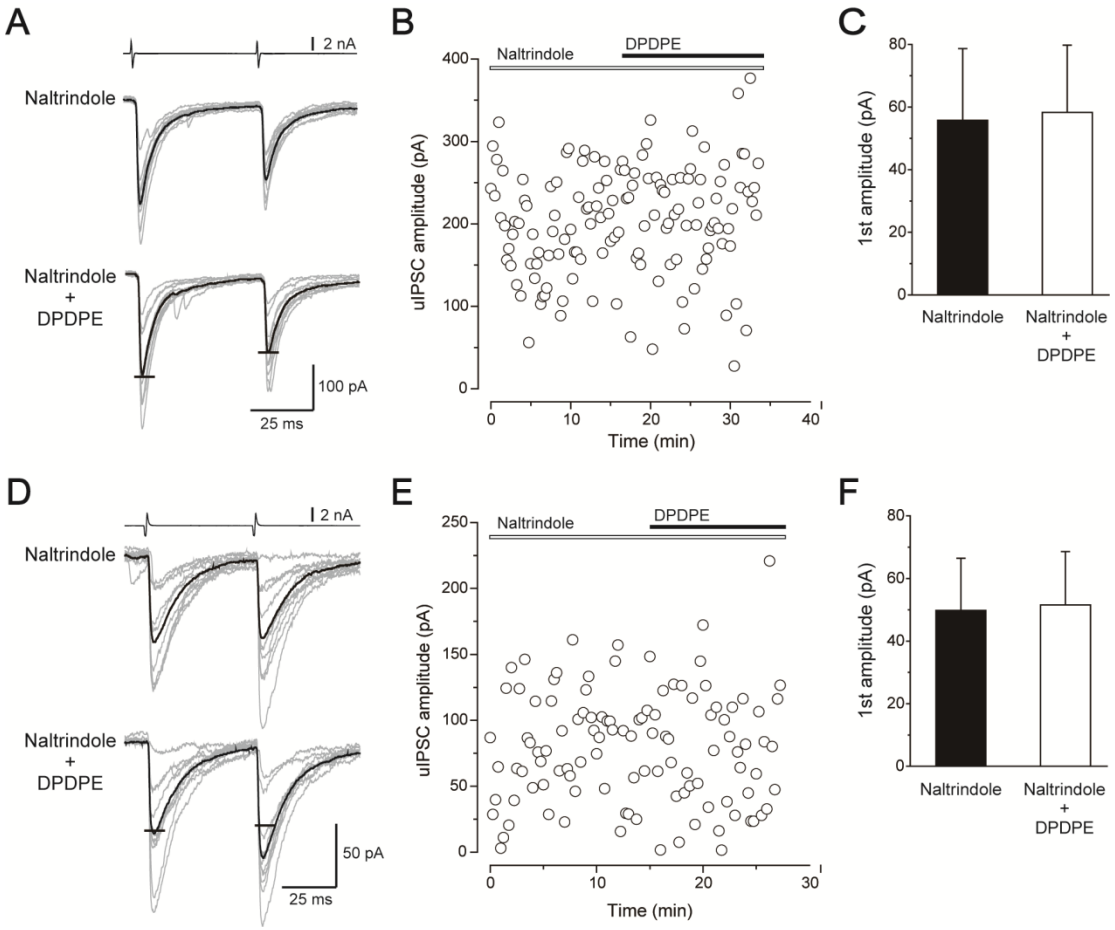

Fig. 7. Effects of DPDPE on uIPSCs obtained from FS→FS (A-C) and FS→Pyr (D-F) connections under application of naltrindole (1 μM). A: uIPSC recordings from postsynaptic FS responding to the injection of paired pulses to presynaptic FS (20 Hz, top trace) before (Naltrindole), and during (Naltrindole + DPDPE) DPDPE application under naltrindole application. Ten consecutive traces (grey) and their average traces (black) are shown. Horizontal bars indicate the amplitude in control. B: Time course of the 1st uIPSC amplitude recorded from the same pairs as in A. C: First uIPSC amplitude in naltrindole, and DPDPE with naltrindole application. D: uIPSC recordings from postsynaptic Pyr responding to the injection of paired pulses to presynaptic FS (20 Hz, top trace) before (Naltrindole), and during (Naltrindole + DPDPE) DPDPE application under naltrindole application. Ten consecutive traces (grey) and their average traces (black) are shown. Horizontal bars indicate the amplitude in control. E: Time course of the 1st uIPSC amplitude recorded from the same pairs as in D. F: First uIPSC amplitude in naltrindole, and DPDPE with naltrindole application. Note that DPDPE had little effect on the amplitude of uIPSCs under application of naltrindole in both FS→FS and FS→Pyr connections

Non-FS→FS and non-FS→Pyr connections show low sensitivity to DPDPE

Effects of DPDPE (1 μM) on the uIPSC amplitude were examined in non-FS→FS/Pyr connections. In contrast to the cases where presynaptic neurons were FS, non-FS→FS connections showed little effect on the uIPSC amplitude (16.1 ± 5.5 pA to 12.6 ± 4.2 pA, n = 6; P = 0.25, paired t-test; Fig. 8A, B, E). Non-FS→Pyr connections also showed little effect on the uIPSC amplitude (13.8 ± 7.7 pA to 14.4 ± 8.6 pA, n = 9; P = 0.71, paired t-test; Fig. 8C-E). PPR and the failure rate were also not affected by DPDPE in non-FS→FS/Pyr connections (Fig. 8E).

These findings of DPDPE obtained from FS/non-FS→FS/Pyr connections suggest that the DOR agonist depresses GABA release from FS but not non-FS.

Little effect of KOR on uIPSCs in FS→FS/Pyr connections

Fig. 9 shows a typical example of uIPSC modulation by U50488, a KOR agonist, in the FS→FS/Pyr connection. U50488 (1 μM) did not significantly change the uIPSC amplitude in FS→FS connections (119.2 ± 25.0 pA to 104.4 ± 18.7 pA, n = 12; P = 0.14, paired t-test; Fig. 9B left) or FS→Pyr connections (114.9 ± 39.3 pA to 100.1 ± 31.8 pA, n = 12; P = 0.16, paired t-test; Fig. 9D left). U50488 affected neither PPR nor failure rate in FS→FS pairs (n = 12): 0.71 ± 0.05 to 0.74 ± 0.06 in PPR (P = 0.73, paired t-test; Fig. 9B middle) and 6.7 ± 3.8% to 7.5 ± 4.5% in failure rate (P = 0.66, Wilcoxon signed-rank test; Fig. 9B right). Similar to FS→FS pairs, FS→Pyr pairs also showed little effect of U50488 on PPR (0.58 ± 0.05 to 0.57 ± 0.06, n = 12; P = 0.95, paired t-test; Fig. 9D middle), and failure rate (5.0 ± 2.6% to 10.0 ± 4.6%, n = 12; P = 0.20, Wilcoxon signed-rank test, Fig. 9D right).

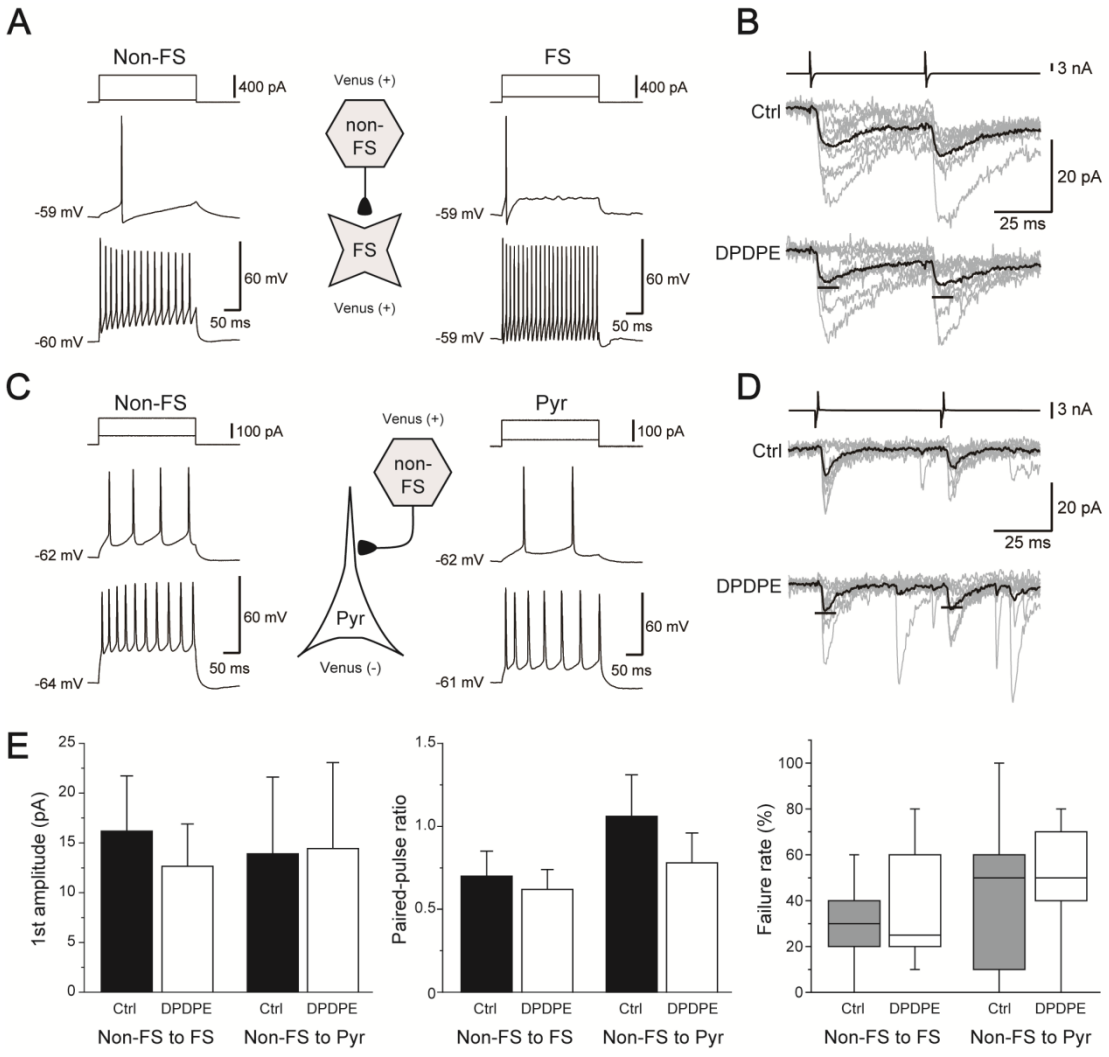

Fig. 8. Effects of DPDPE on uIPSCs obtained from non-FS→FS and non-FS→Pyr connections. A, C: Recording from non-FS and FS (A) and non-FS and Pyr (C) in layer V IC. Both non-FS exhibited regular spike firing with adaptation. B, D: uIPSC recordings from FS (B; same cells shown in A) and Pyr (D; same cells shown in C) before (Ctrl) and during 1 μM DPDPE application. Note that DPDPE had little effect on uIPSCs. E: First uIPSC amplitude (left), PPR (middle), and failure rate of 1st uIPSCs (right) in control and during DPDPE application in non-FS→FS and in non-FS→Pyr connections. Failure rate was represented by a box-and-whisker plot.

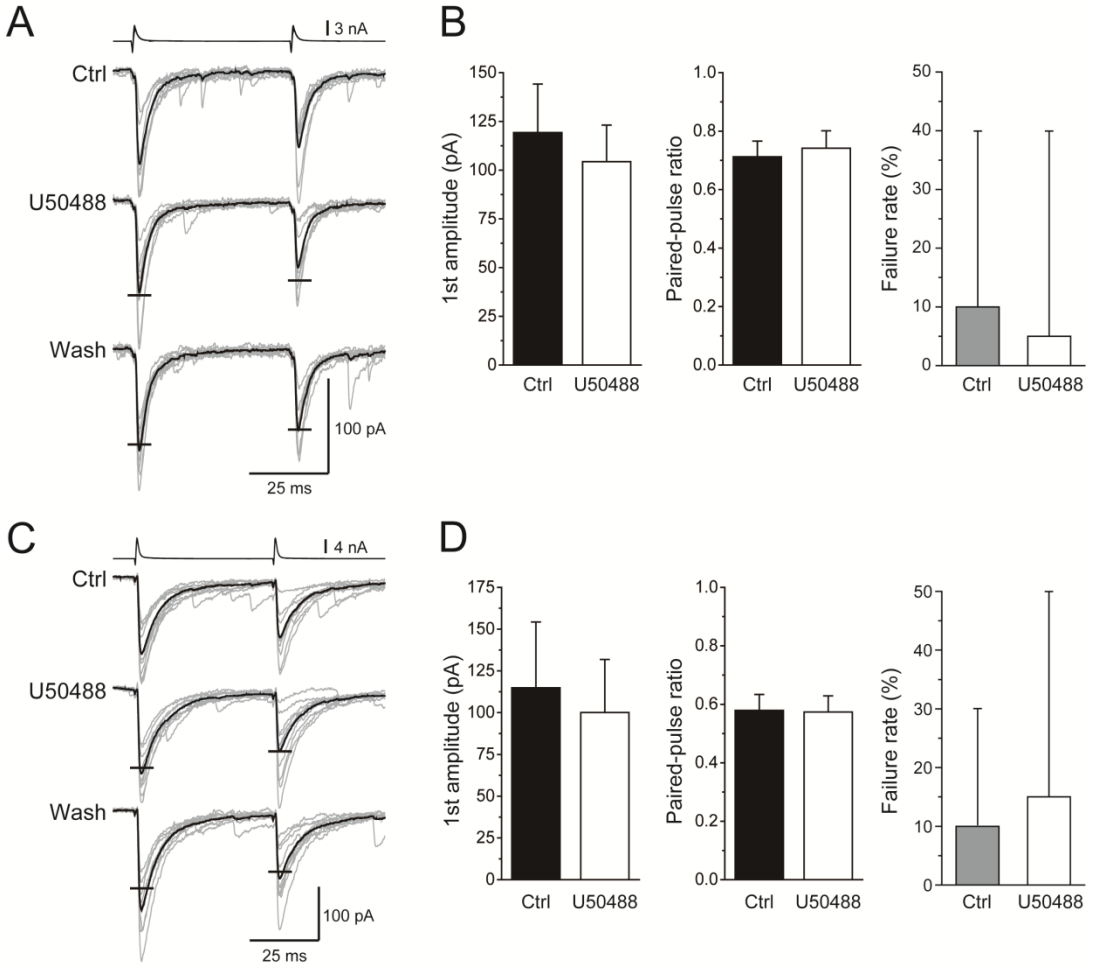

Fig. 9. Small effect of U50488 on uIPSCs obtained from FS→FS/Pyr connections. A: uIPSC recordings from postsynaptic FS responding to the injection of paired pulses to presynaptic FS (20 Hz, top trace) before (Ctrl), during (U50488), and after (Wash) U50488 (1 μM) application. Ten consecutive traces (grey) and their average traces (black) are shown. Horizontal bars indicate the amplitude in control. Note that FS had little effect of U50488 on uIPSCs. B: First uIPSC amplitude (left), PPR (middle), and failure rate of 1st uIPSCs (right) in control and during U50488 application. Note that U50488 did not significantly change 1st uIPSC amplitude, PPR, or failure rate. C: uIPSC recordings from Pyr responding to the injection of paired pulses to presynaptic FS (20 Hz, top trace) before (Ctrl), during (U50488), and after (Wash) U50488 (1 μM) application. Ten consecutive traces (grey) and their average traces (black) are shown. Bars indicate the amplitude in control. Note that Pyr showed little effect of U50488 on uIPSCs. D: First uIPSC amplitude (left), PPR (middle), and failure rate of 1st uIPSCs (right) in control and during U50488 application. Failure rate was represented by a box-and-whisker plot. Note U50488 did not significantly change 1st uIPSC amplitude, PPR, or failure rate of 1st uIPSCs.

Discussion

The present study focused on the functional roles of opioids in inhibitory synaptic transmission in the IC. Differential modulatory mechanisms of MOR and DOR activation to be dependent upon postsynaptic neuronal subtypes were investigated. DAMGO reduced uIPSC amplitude in FS/non-FS→FS but not FS/non-FS→Pyr connections, whereas DPDPE consistently reduced uIPSC amplitude in FS→FS/Pyr connections without significant effects on non-FS→FS/Pyr connections. These differential modulations of cortical activities may explain the MOR-dominant suppression of pain.

Postsynaptic cell-type-dependent modulation by MOR

It has been known that MOR activation suppresses excitatory synaptic transmission in the cerebral cortex via presynaptic mechanisms (Tanaka and North, 1994; Zheng, 2010). The present study provides the evidence that MOR depresses the specific inhibitory synaptic transmission, FS/non-FS→FS connections, and this depression is likely mediated by presynaptic mechanisms. In contrast, uIPSCs in FS/non-FS→Pyr connections were not affected by DAMGO, which corroborates the finding of a minimal effect of DAMGO on evoked IPSC recorded from ACC Pyr (Tanaka and North, 1994). These MOR-induced modulation mechanisms of inhibitory synaptic transmission result in increased inhibition to Pyr. In the IC, $GABA_A$-mediated inhibitory synaptic transmission plays a pivotal role in the regulation of excitatory propagation as AMPA receptor-mediated excitatory synaptic transmission (Fujita et al., 2010). Therefore, findings of synaptic transmission are consistent with the DAMGO-induced depression of excitatory propagation in the IC (see Chapter II).

Opioidergic receptors are coupled to Gi/o, which inhibits producing cyclic AMP. The present study focused on their action to $GABA_A$ receptors, however, G-protein coupled receptors regulate other receptors and ion channels. It has to be noted that opioidergic modulation of $GABA_A$ is not the only mechanism that regulates IC activities.

Presynaptic cell-type-dependent modulation by DOR

In contrast to differential regulation of uIPSCs by MOR, the activation of DOR reduced uIPSC amplitude in FS→FS and FS→Pyr connections. These findings are compatible with the report of DPDPE-induced depression of evoked IPSCs in the ACC (Tanaka and North, 1994). These suppressive effects of DOR seem to induce a controversial function. That is, the reduction of uIPSCs in FS→FS connections increases in inhibition reduces disinhibition, while FS→Pyr depression is likely to facilitate neural activities of Pyr. DOR is thought to suppress excitatory synaptic transmission onto Pyr (Tanaka and North, 1994), which seems to contradict the finding of the depression of FS→Pyr connections. However, optical imaging data indicates the slight facilitation of excitatory propagation (see Chapter II); therefore, FS→Pyr connections play a key role in regulating excitation in the IC. Although there may be an endogenous mechanism that disinhibits Pyr without activating the FS→FS connections via DORs, the present data do not completely support this idea that DORs are entirely facilitating. On the other hand, DPDPE had little effect on uIPSCs in non-FS→FS/Pyr connections. As presynaptic FS showed higher connection rate with larger amplitude of uIPSC that non-FS, it is considered that effects of DOR activation on inhibitory synaptic transmission are dominant in FS→FS and FS→Pyr connections.

DAMGO-induced decreases in uIPSC amplitude was accompanied with an increase in failure rate and without changes in uIPSC kinetics in FS/non-FS→FS connections. Similarly, DPDPE depressed uIPSCs without an increase in PPR in FS→Pyr connections. These findings looks to be discrepant to the idea that μ and δ agonists target to presynaptic sites. However, short term plasticity is not necessarily sensitive to the presynaptic modulation

(Almado et al., 2012), and therefore, the hypothesis described above is reasonable.

Minor role of KOR in GABAergic synaptic transmission

KOR agonists also have antinociceptive effects (Fields, 2004). One of their principal mechanisms is disinhibition of pain inhibitory neurons by reducing excitatory inputs in the rostral ventromedial medulla (Ackley et al., 2001). On the other hand, reduction of IPSCs by KOR activation has been observed in the central amygdala (Gilpin et al., 2014) and the bed nucleus of the stria terminalis (Li et al., 2012). The present results demonstrated that a KOR agonist had little effect on uIPSCs, which is consistent with the anatomical evidence that the IC shows low expression of KORs (Burkey et al., 1996). Taken together, agonists of KOR are likely to exert antinociceptive actions in the subcortical regions. The difference in action sites between MOR and KOR might result in a corresponding difference in their strength as analgesic drugs.

Functional roles of cortical opioid receptors in pain regulation

Physiological functions of the IC for nociceptive information processing have been explored using both anatomical and electrophysiological approaches (Burkey et al., 1996, 1999; Treede et al., 2000; Ostrowsky et al., 2002; Jasmin et al., 2003, 2004). This issue is critical to the understanding of the mechanisms of opioid receptor-mediated analgesia and remains controversial. Among these studies, many have reported that IC suppression causes analgesia. Jasmin et al. (2003), for instance, reported that topical increase in GABA by using an enzyme inhibitor or gene transfer mediated by a viral vector produced lasting analgesia by enhancing the descending inhibition of spinal nociceptive neurons. In addition, direct electrical stimulation of the IC performed in patients with drug refractory temporal lobe epilepsy, using stereotactically implanted depth electrodes, elicited painful sensations (Ostrowsky et al., 2002). Ostrowsky et al. (2002) also reported that painful responses could never be obtained when stimulating S2 directly using identical stimulation parameters. Thus, the activation of the IC is likely to facilitate nociception. In contrast, the activation of the surrounding cortices of the IC, involving the motor cortex (Senapati et al., 2005a; Viisanen and Pertovaara, 2010; Viisanen et al., 2012; Cha et al., 2013; França et al., 2013), the primary (Senapati et al., 2005c; Malmierca et al., 2012) and secondary somatosensory cortices (Kuroda et al., 2000, 2001; Malmierca et al., 2012; S1 and S2, respectively), and ACC (Senapati et al., 2005b), facilitates descending inhibition, and as a result, weakens nociception.

The present findings are in line with this idea. First, an MOR agonist is the most potent pain killer and suppresses excitatory propagation in the IC. However, the smaller effect of KOR activation on inhibitory synaptic transmission is also consistent with clinical findings of a smaller effect of a KOR agonist on nociception. According to the above hypothesis, the facilitative effect of DOR activation might work to potentiate the intensity of nociception, which might then be a possible reason for the previous findings showing that DOR activation

had little effect on acute pain (Gavériaux-Ruff and Kieffer, 2011; Pradhan et al., 2011). DOR densely expresses in the striatum and lateral reticular nucleus in addition to the cerebral cortex (Mansour et al., 1995), and these DORs might partially antagonize the facilitation of the IC activities. This might be a reason for less potency as a pain killer (Gavériaux-Ruff and Kieffer, 2011; Pradhan et al., 2011; Chu Sin Chung and Kieffer, 2013) in comparison to MOR.

Nociceptive stimuli to dental pulps or periodontal ligaments induce excitation in the IC with topographically organization have demonstrated (Horinuki et al., 2015, 2016; Nakamura et al., 2015, 2016). In addition to nociceptive information, surrounding regions in the IC receive other sensation modalities such as thermal, gustatory, and visceral sensations (Cechetto and Saper, 1987; Yamamoto et al., 1988; Allen et al., 1991; Nakashima et al., 2000; Jasmin et al., 2004). Taking into account the evidence that the IC receives limbic structures from the amygdala, infralimbic cortex, and ACC (Shi and Cassell, 1998), the IC is likely to integrate sensory information from multiple inputs, especially those in the oral cavity, with emotion (Kobayashi, 2011). In this notion, MOR-induced depression and DOR-induced facilitation of excitatory propagation in the IC may induce contradictory modulation of emotional behaviors. Indeed, a behavioral study has reported contradictory emotional responses in MOR/DOR knockout mice (Filliol et al., 2000).

CHAPTER II

Opposite effects of mu and delta opioid receptor agonists on excitatory propagation induced in rat somatosensory and insular cortices by dental pulp stimulation

Introduction

The IC receives multisensory information, e.g., gustation, viscerosensation, and audition (Yamamoto et al., 1984; Cechetto and Saper, 1987; Yasui et al., 1991; Rodgers et al., 2008). In addition to these multiple types of sensation, the IC plays a pivotal role in nociception. Stimulation of the agranular IC, the ventral part of the IC, suppresses nociceptive responses via modulating neural activities of the dorsal raphe nucleus, periaqueductal gray, and parabrachial nucleus (Jasmin et al., 2004). In terms of orofacial nociception, insular oral region (IOR) and the dorsally adjacent S2, which are located caudal to the middle cerebral artery (MCA) in the rat, respond to electrical stimulation of dental pulps (Shigenaga et al., 1974; Nakamura et al., 2015, 2016) or periodontal ligaments (Horinuki et al., 2015, 2016). S2/IOR is likely to encode the strength of nociception because the amplitude of excitation in S2/IOR is dependent on the intensity of molar pulp stimulation (Nakamura et al., 2015). Several anatomical studies have demonstrated that the subregions of the IC send projections to the trigeminal caudal and oral subnuclei (Yasui et al., 1991; Desbois et al., 1999; Sato et al., 2013), which receive nociceptive primary afferents from the orofacial area (for review see Bereiter et al., 2000; Sessle, 2006).

Morphine is one of the most effective pain killers (Akil et al., 1998; Kieffer et al., 2002), and its receptors, opioid receptors, are classified into MOR, KOR, and DOR subtypes. IC neurons express all subtypes of opioid receptors (Mansour et al., 1995; Svingos et al., 1995; Burkey et al., 1996); however, anatomical analysis of the IC shows low expression of KORs (Burkey et al., 1996). Among these opioid receptors, MOR is a principal target of analgesics (Akil et al., 1998; Kieffer et al., 2002). Indeed, microinjection of morphine into the IC reduces responses of dorsal horn neurons to noxious thermal stimuli (Burkey et al., 1996). A possible mechanism for the reduction of the noxious response is a suppressive effect of MOR agonists on excitatory synaptic transmission in the cerebral cortex (Tanaka and North, 1994; Zheng, 2010). In contrast, DOR contributes to chronic pain and to brain disorders such as addiction and seizures rather than to acute nociception (Pradhan et al., 2011; Chu Sin Chung and Kieffer, 2013). Interestingly, mice deficient in MOR or DOR exhibit opposite effects on mood state (Filliol et al., 2000). Therefore, it is likely that MOR and DOR differentially modulate cortical functions, but little information is available regarding their contradictory roles.

In the present study, optical imaging using a voltage-sensitive dye was performed to compare the effects of MOR, DOR, and KOR agonists on cortical excitatory propagation *in vivo* in response to dental pulp stimulation.

Materials and Methods

The Institutional Animal Care and Use Committee at Nihon University approved the study protocol, and all experiments were performed in accordance with the National Institutes of Health Guide for the Care and Use of Laboratory Animals. All efforts were made to minimize the number of animals used as well as their suffering.

Preparation of animals

Six- to seven-week-old male Sprague-Dawley rats (Sankyo Labo, Tokyo, Japan) weighing 214.8 ± 5.4 g (n = 29) were injected with atropine methyl bromide (5 mg/kg, i.p.) and urethane (1.5 g/kg, i.p.). The efficacy of anesthesia was gauged by the absence of a toe pinch reflex, and additional urethane was added as needed. Body temperature was monitored using a rectal probe (BWT-100, Bio Research Center, Osaka, Japan) and was maintained at ~37˚C using a heating pad. Lidocaine (2% gel, AstraZeneca, Tokyo, Japan) was administered to the incisions. The animal was tilted 60˚ laterally, and the left temporal muscle and zygomatic arch were carefully removed. A craniotomy was performed to image the surface of S1 and S2/IOR using a CCD camera (MiCAM02, Brainvision, Tokyo, Japan).

Bipolar electrodes made from an enamel-coated copper wire (diameter = 80 μm) were inserted into the right maxillary 1st molar pulp. The tip of the wire (0.5-1.0 mm) was bared and fixed with dental cement (Estelite Flow Quick, Tokuyama Dental, Tokyo, Japan).

Optical imaging

RH1691 (1 mg/ml, Optical Imaging, New York, USA) was dissolved in 0.9% saline and applied to the cortical surface for approximately 1 hr. Fluorescent changes in RH1691 were measured using the CCD camera system mounted on a stereomicroscope (Leica Microsystems, Wetzlar, Germany). The cortical surface was illuminated through a 632 nm excitation filter and a dichroic mirror using a tungsten-halogen lamp (CLS150XD, Leica Microsystems). The fluorescent emission was captured through an absorption filter ($\lambda > 650$ nm long-pass, Andover, Salem, USA). The CCD camera had a 6.4 × 4.8 mm^2 imaging area consisting of 184 × 124 pixels.

To remove signals due to acute bleaching of the dye, values in the absence of any stimuli were subtracted from each recording. Each image was constructed from paired recordings with and without stimulation. The sampling interval was 4 ms, and the acquisition time was 500 ms. Forty consecutive images in response to the stimuli were averaged to reduce the noise described above.

Electrical stimulation and drug application

For electrical stimulation, voltage pulses of 100 μs duration with amplitudes of 5 V were applied using a stimulator unit (STG2008, Multi Channel Systems, Reutlingen, Germany). In the present study, 5 voltage pulses at 50 Hz were applied at 0.05 Hz to obtain stable optical responses.

The MOR agonist DAMGO (10-100 μM), the DOR agonist DPDPE (10-100 μM), or the KOR agonist U50488 (10-100 μM) was directly applied to the cortical surface. It is considered that this application method allows the drugs to penetrate at least into the superficial layers (layers I-III), where application of voltage-sensitive dyes via the same method shows a sufficient penetration, as described in the previous study (Nakamura et al., 2015; Fujita et al., 2010). In addition, the same method for application of 6-Cyano-7-nitroquinoxaline-2,3-dione (CNQX) effectively suppresses excitatory propagation in the cortex (Fujita et al., 2010), indicating a sufficient blockade of AMPA receptors.

Data analysis

In the optical imaging, the changes in the intensity of fluorescence (ΔF) of each pixel relative to the initial intensity of fluorescence (F) were calculated (ΔF/F), and the ratio was processed with a spatial filter (9 × 9 pixels). A significant response was defined as a signal exceeding 7 times the standard deviation of the baseline noise. The optical imaging data were processed and analyzed using a software program (Brain Vision Analyzer, Brainvision LLC, Morrisville, USA). Images were aligned across multiple rats using the rhinal fissure and MCA as markers.

The spatial profiles of excitation using the initial and maximum responses were estimated. The initial response was obtained by outlining the evoked excitation in the first frame that exhibited a significant increase in the optical signal. The maximum response was defined as the outline of the excitatory response in the frame containing the maximum amplitude of the optical signal in the center of the initial response, at the time when the largest amplitude was obtained. Rise and decay time were measured from 10% to the peak and from 80% to 20% of the peak amplitude, respectively.

Statistics

The data are presented as the mean ± standard error of the mean. Optical responses to the maxillary molar pulp stimulation between control and DAMGO/DPDPE/U50488 application were also compared by paired *t*-tests with the Bonferroni correction. The area of the maximum responses was not statistically analyzed because the excitation often expanded out of the frame. As an alternative, the area in which the maximum responses overlapped in ≥ 50% of rats was outlined. $P < 0.025$ was considered significant.

Results

Cortical excitatory propagation responding to the maxillary molar pulp stimulation

Electrical stimulation of the maxillary molar pulp (5 pulse-trains at 50 Hz, 5 V) initially evoked excitation along the border of S2 and IOR, immediately caudal to the MCA (Fig. 1A). Just after S2/IOR excitation, another focal excitation occurred in S1. The focal excitation then expanded concentrically, reaching a peak at 18.0 ± 2.1 ms (n = 29) after stimulation.

Next, the effects of MOR, DOR, or KOR activation on excitatory propagation in S2/IOR in response to the maxillary molar pulp stimulation were examined (Nakamura et al., 2015, 2016).

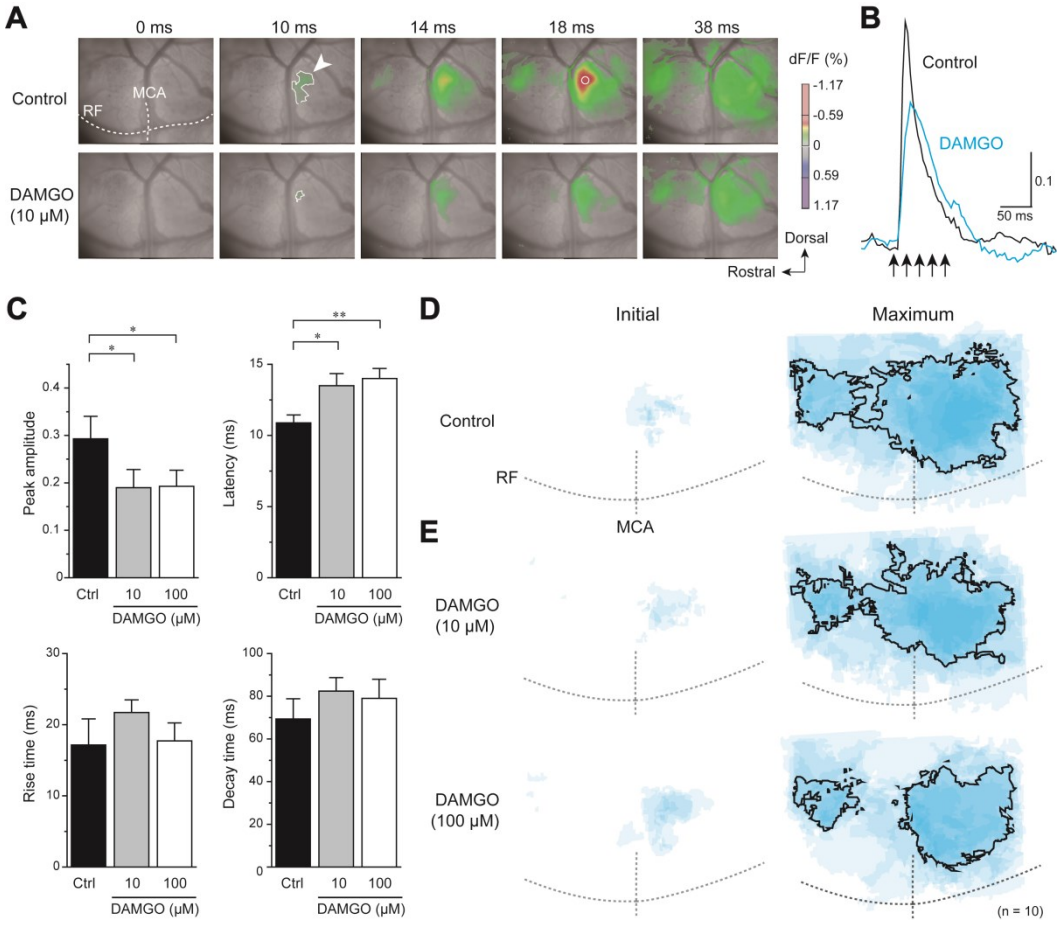

Fig. 1. Effects of DAMGO on cortical excitatory propagation induced by repetitive electrical stimulation (5 pulses at 50 Hz) of the upper molar pulp. A: Color-coded optical signals induced by electrical stimulation at baseline (upper panels) and during application of 10 μM DAMGO (lower panels). Excitation was first induced in S2/IOR (arrowhead) 10 ms after the first electrical stimulation and then expanded concentrically toward the surrounding cortices, including S1 and S2. Note that DAMGO suppressed the optical signal amplitude obtained from the region of interest (ROI; white circle in the center of the largest excitation). The time from stimulation onset (arrow) is shown in the upper panels. B: Optical responses obtained from the ROI (A) under control conditions (black) and during DAMGO application (blue). C: Peak amplitude, latency, rise time, and decay time under control conditions (black) and during DAMGO application (gray and white). Note the DAMGO-induced suppression of amplitude and the longer latency (n = 10). D, E: The initial (left) and maximum (right) responses under control conditions (D) and during DAMGO application (E) were superimposed with reference to the MCA and rhinal fissure (RF). The number of overlapping responses is represented by the gradation of colors; the area painted with the deepest color showed responses in all animals. For the maximum responses, the area showing overlap in 5/10 rats is outlined with solid lines. *: $P < 0.025$, **: $P < 0.005$, paired t-test with the Bonferroni correction.

MOR suppresses cortical excitatory propagation

The application of 10 μM DAMGO to the IC surface suppressed the excitatory propagation in S2/IOR. DAMGO decreased the peak amplitude of optical signals in the center of excitation from 0.29 ± 0.05 to 0.19 ± 0.04 (n = 10; P < 0.025, paired t-test; Fig. 1A-C). In addition, DAMGO delayed the latency of excitation from stimulation: 10.9 ± 0.6 ms in control and 13.5 ± 0.9 ms during DAMGO application (n = 10; P < 0.01, paired t-test; Fig. 1C). In contrast, DAMGO had little effect on the rise time and decay time, as shown in Fig. 1C. The initially excited region was almost unchanged by DAMGO (Fig. 1D, E left), whereas the maximum area was shrunk by DAMGO (Fig. 1D, E right). Similar modulatory effects on the optical signal kinetics were observed during application of 100 μM DAMGO (Fig. 1C-E).

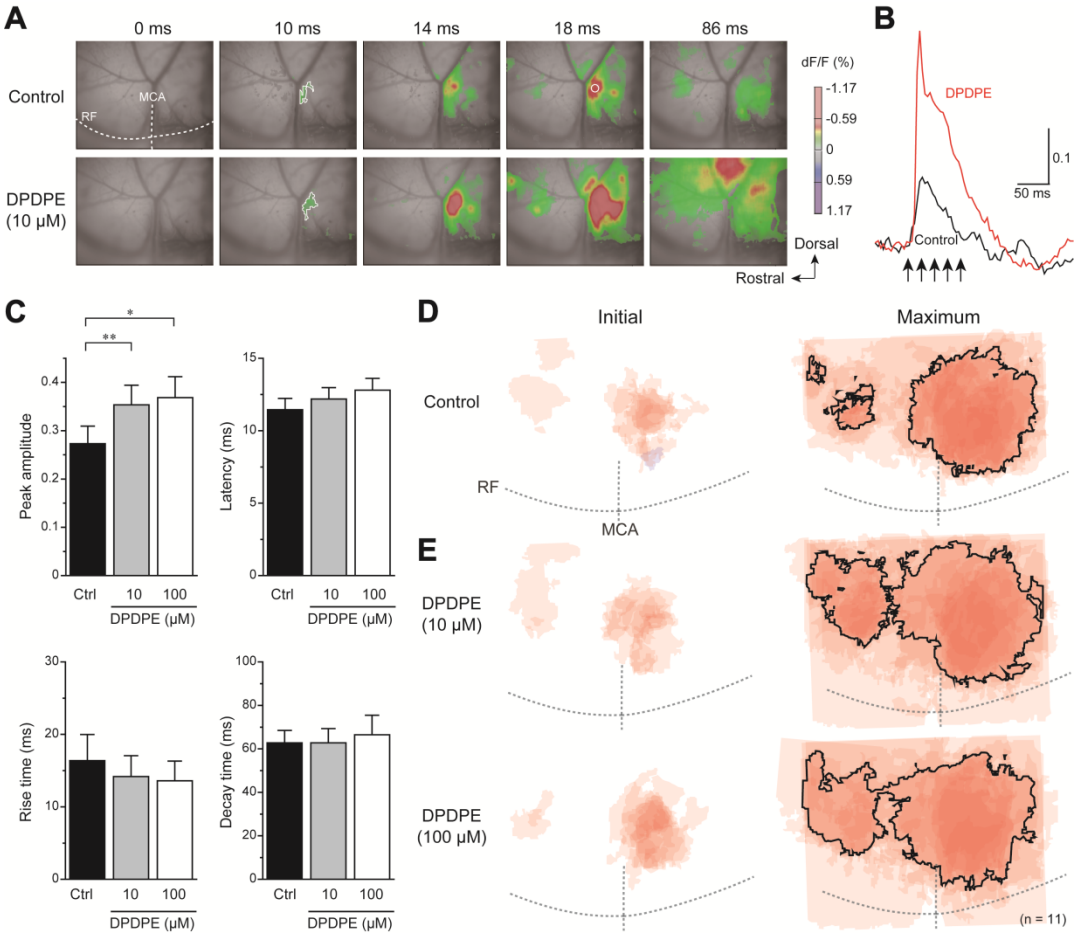

Fig. 2. Effects of DPDPE on cortical excitatory propagation induced by repetitive electrical stimulation of the upper molar pulp. A: Optical signals induced by electrical stimulation in control (upper panels) and during application of 10 μM DPDPE (lower panels). Note that DAMGO suppressed the optical signal amplitude obtained from the ROI (white circle). B: Optical responses obtained from the ROI (A) under control conditions (black) and during DPDPE application (red). C: Peak amplitude, latency, rise time, and decay time under control conditions (black) and during DPDPE application (gray and white). Note the DPDPE-induced increase in amplitude (n = 11). D, E: The initial (left) and maximum responses (right) under control conditions (D) and during DPDPE application (E) were superimposed with reference to the MCA and RF. In the maximum responses, the area showing overlap in 6/11 rats is outlined with solid lines. *: P < 0.025, **: P < 0.005, paired t-test with the Bonferroni correction.

DOR enhances cortical excitatory propagation

The application of 10 μM DPDPE, in contrast, increased the peak amplitude from 0.27 ± 0.04 to 0.35 ± 0.04 (n = 11; P < 0.01, paired t-test; Fig. 2A-C) without significant changes in the latency, rise time or decay time (Fig. 2C). Similar to the results obtained from DAMGO application, the initially excited region was almost unchanged by DPDPE (Fig. 2D, E left). However, the maximum area was expanded by DPDPE (Fig. 2D, E right). These modulatory effects on the optical signal kinetics were observed during application of 100 μM DPDPE (Fig. 2C, D).

Together, these results point to contradictory effects of MOR and DOR on cortical excitation at the macroscopic level.

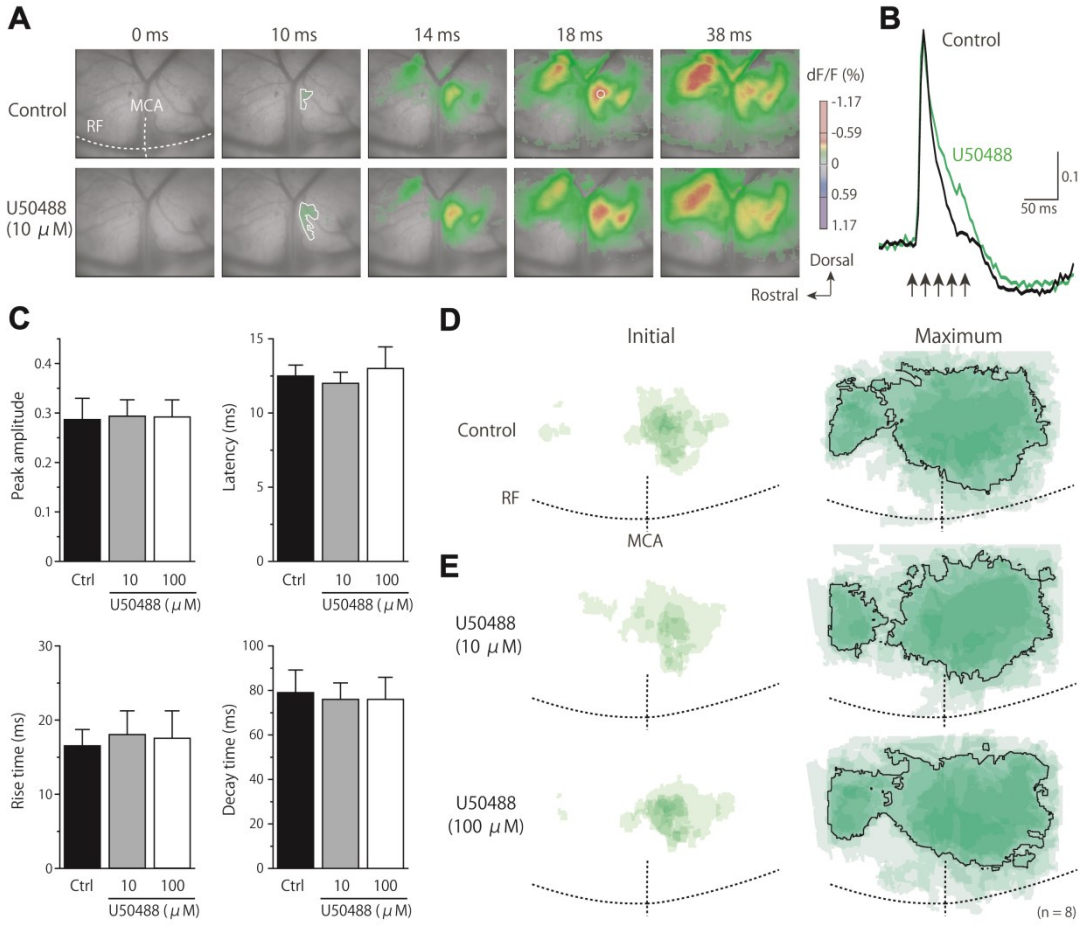

Fig. 3. Little effect of U50488 on cortical excitatory propagation induced by the upper molar pulp stimulation. A: Optical signals in control (upper panels) and during application of 10 μM U50488 (lower panels). Note little effect of U50488 on the optical signal. B: Optical responses obtained from the ROI (A) under control conditions (black) and during U50488 application (green). C: Peak amplitude, latency, rise time, and decay time under control conditions (black) and during U50488 application (gray and white, n = 8). D, E: The initial (left) and maximum responses (right) under control conditions (D) and during U50488 application (E) were superimposed with reference to the MCA and RF. In the maximum responses, the area showing overlap in 4/8 rats is outlined with solid lines.

KOR has little effect on cortical excitatory propagation

U50488 (10-100 μM), an agonist of KOR, had little on the properties of excitatory propagation (Fig. 3). Any properties including the peak amplitude, latency, rise time, and

decay time were not significantly changed by application of U50488 (n = 8; P > 0.1, paired t-test; Fig. 3C). In addition, the initial and maximum areas of cortical excitation were not affected by U50488 (Fig. 3D).

Discussion

Suppressive effects of DAMGO on cortical excitatory propagation

Considering our previous optical imaging study showing that an antagonist of AMPA receptors diminishes most part of the cortical excitatory propagation in the rat IC (Fujita et al., 2010), excitatory synaptic transmission plays a pivotal role in excitatory propagation in the IC. Therefore, the DAMGO-induced suppression of excitatory propagation in this study is likely to be principally mediated by modulation of glutamatergic synaptic transmission. This view is supported by several lines of evidence obtained from *in vitro* electrophysiological studies: MOR activation suppresses excitatory synaptic transmission in the rat cerebral cortex via presynaptic mechanisms (Tanaka and North, 1994; Zheng, 2010), and DAMGO has little effect on evoked IPSCs recorded from pyramidal cells (Pyr; Tanaka and North, 1994).

Electrophysiological and functional imaging studies have demonstrated that nociceptive stimuli activate IC neurons; however, the role of IC excitation has remained controversial. IC suppression by increasing the content of GABA induces analgesia in the rat (Jasmin et al., 2003), and electrical stimulation of the IC performed in patients with drug-refractory temporal lobe epilepsy induces painful sensations (Ostrowsky et al., 2002), suggesting that IC activation facilitates nociception. In contrast, the activation of the cortices surrounding the IC, specifically the rat motor cortex (Senapati et al., 2005a; Viisanen et al., 2010, 2012; Cha et al., 2013; Franca et al., 2013), S1 (Senapati et al., 2005c; Malmierca et al., 2012), S2 (Malmierca et al., 2012; Kuroda et al., 2001) and anterior cingulate cortex (Senapati et al., 2005b), facilitates descending inhibition, and thus weakens nociception. The present finding of the MOR-mediated suppression of excitatory propagation in S2/IOR may hint at the answer to the above question. Considering the fact that microinjection of morphine into the rat IC reduces the responses of dorsal horn neurons to noxious thermal stimuli (Burkey et al., 1996), IC activation may facilitate nociception.

Facilitative effects of DPDPE on cortical excitatory propagation

At the synaptic level, the role of DORs has been controversial in the cerebral cortex. Tanaka and North (1994) report that DOR activation suppresses evoked EPSCs that are recorded from the rat anterior cingulate Pyr. However, they also report the suppression of evoked IPSCs (Tanaka and North, 1994). In the IC, the suppressive effects of inhibitory synaptic transmission from fast-spiking interneurons to Pyr by DPDPE have found (see Chapter I). Therefore, the present optical imaging data, the facilitation of excitatory propagation by DPDPE, might be induced by suppression of inhibition on Pyr.

According to the above hypothesis, the facilitative effect of DORs on IC excitation might potentiate the intensity of nociception. DORs are densely expressed in the striatum and lateral reticular nucleus in addition to the rat cerebral cortex (Mansour et al., 1995), and these DORs might antagonize the facilitation of the IC activities. Therefore, DOR-induced facilitation of IC excitation is at least partially consistent with the previous findings that DOR activation has little effect on acute pain (Pradhan et al., 2011; Gaveriaux-Ruff and Kieffer, 2011). This is a possible reason for the lower potency of DOR agonists as pain killers (Pradhan et al., 2011; Chu Sin Chung and Kieffer, 2013; Gaveriaux-Ruff and Kieffer, 2011) in comparison to MOR agonists.

In contrast to the DAMGO and DPDPE, U50488 did not significantly change the profiles of IC excitation. This finding is consistent with the previous study that reports low expression of KORs in the IC (Burkey et al., 1996).

Opioidergic modulation of the limbic system

In addition to the multiple sensory inputs, IC receives the projections from the limbic structures including the amygdala and infralimbic and anterior cingulate cortices (Shi and Cassell, 1998). The IC plays roles in processing emotion, as recently reported (Craig, 2009). Kieffer and his colleagues have demonstrated that DORs are an attractive target for the treatment of chronic pain and mood disorders (Pradhan et al., 2011; Chu Sin Chung and Kieffer, 2013; Gaveriaux-Ruff and Kieffer, 2011). In this context, MOR-induced suppression and DOR-induced facilitation of excitatory propagation in the IC may induce contradictory modulation of emotional behaviors. Indeed, a behavioral study has reported contradictory emotional responses in MOR/DOR knockout mice (Filliol et al., 2000).

Conclusion

The present study focused on the functional roles of opioids in inhibitory synaptic transmission in the IC. I investigated the differential modulatory mechanisms of MOR and DOR activation dependent upon postsynaptic neuronal subtypes. DAMGO suppressed uIPSC amplitude in FS/non-FS→FS but not FS/non-FS→Pyr connections, whereas DPDPE consistently suppressed uIPSC amplitude in FS→FS/Pyr connections. In addition, the optical imaging demonstrated a suppressive effect of MOR and a facilitative effect of DOR on cortical excitatory propagation. These differential modulations of cortical activities may explain the MOR-dominant suppression of acute pain.

Acknowledgements

I am grateful to Prof. Oi for the opportunity to perform this study, Prof. Kobayashi and Assis. Prof. Koyanagi for their instructions of this study, and colleagues in Department of Pharmacology for their technical advice and assistance.

References

Ackley MA, Hurley RW, Virnich DE, Hammond DL (2001) A cellular mechanism for the antinociceptive effect of a kappa opioid receptor agonist. Pain 91:377-388.

Akil H, Owens C, Gutstein H, Taylor L, Curran E, Watson S (1998) Endogenous opioids: overview and current issues. Drug Alcohol Depend 51:127-140.

Allen GV, Saper CB, Hurley KM, Cechetto DF (1991) Organization of visceral and limbic connections in the insular cortex of the rat. J Comp Neurol 311:1-16.

Almado CE, Machado BH, Leão RM (2012) Chronic intermittent hypoxia depresses afferent neurotransmission in NTS neurons by a reduction in the number of active synapses. J Neurosci 32:16736-16746.

Bereiter DA, Hirata H, Hu JW (2000) Trigeminal subnucleus caudalis: beyond homologies with the spinal dorsal horn. Pain 88:221-224.

Burkey AR, Carstens E, Wenniger JJ, Tang J, Jasmin L (1996) An opioidergic cortical antinociception triggering site in the agranular insular cortex of the rat that contributes to morphine antinociception. J Neurosci 16:6612-6623.

Burkey AR, Carstens E, Jasmin L (1999) Dopamine reuptake inhibition in the rostral agranular insular cortex produces antinociception. J Neurosci 19:4169-4179.

Cechetto DF, Saper CB (1987) Evidence for a viscerotopic sensory representation in the cortex and thalamus in the rat. J Comp Neurol 262:27-45.

Cha M, Ji Y, Masri R (2013) Motor cortex stimulation activates the incertothalamic pathway in an animal model of spinal cord injury. J Pain 14:260-269.

Chu Sin Chung P, Kieffer BL (2013) Delta opioid receptors in brain function and diseases. Pharmacol Ther 140:112-120.

Coffeen U, Lopez-Avila A, Ortega-Legaspi JM, del Angel R, Lopez-Munoz FJ, Pellicer F (2008) Dopamine receptors in the anterior insular cortex modulate long-term nociception in the rat. Eur J Pain 12:535-543.

Coffeen U, Manuel Ortega-Legaspi J, Lopez-Munoz FJ, Simon-Arceo K, Jaimes O, Pellicer F (2011) Insular cortex lesion diminishes neuropathic and inflammatory pain-like behaviours. Eur J Pain 15:132-138.

Craig AD (2009) How do you feel--now? The anterior insula and human awareness. Nat Rev Neurosci 10:59-70.

Desbois C, Le Bars D, Villanueva L (1999) Organization of cortical projections to the medullary subnucleus reticularis dorsalis: a retrograde and anterograde tracing study in the rat. J Comp Neurol 410:178-196.

Fields H (2004) State-dependent opioid control of pain. Nat Rev Neurosci 5:565-575.

Filliol D, Ghozland S, Chluba J, Martin M, Matthes HW, Simonin F, Befort K, Gavériaux-Ruff C, Dierich A, LeMeur M, Valverde O, Maldonado R, Kieffer BL (2000) Mice deficient for δ- and μ-opioid receptors exhibit opposing alterations of emotional responses. Nat Genet 25:195-200.

França NR, Toniolo EF, Franciosi AC, Alves AS, de Andrade DC, Fonoff ET, Britto LR, Dale CS (2013) Antinociception induced by motor cortex stimulation: somatotopy of behavioral response and profile of neuronal activation. Behav Brain Res 250:211-221.

Fujita S, Adachi K, Koshikawa N, Kobayashi M (2010) Spatiotemporal dynamics of excitation in rat insular cortex: intrinsic corticocortical circuit regulates caudal-rostro excitatory propagation from the insular to frontal cortex. Neuroscience 165:278-292.

Gavériaux-Ruff C, Kieffer BL (2011) Delta opioid receptor analgesia: recent contributions from pharmacology and molecular approaches. Behav Pharmacol 22:405-414.

Gilpin NW, Roberto M, Koob GF, Schweitzer P (2014) Kappa opioid receptor activation decreases inhibitory transmission and antagonizes alcohol effects in rat central amygdala. Neuropharmacology 77:294-302.

Horinuki E, Shinoda M, Shimizu N, Koshikawa N, Kobayashi M (2015) Orthodontic force facilitates cortical responses to periodontal stimulation. J Dent Res 94:1158-1166.

Horinuki E, Yamamoto K, Shimizu N, Koshikawa N, Kobayashi M (2016) Sequential Changes in Cortical Excitation during Orthodontic Treatment. J Dent Res 95:897-905.

Jasmin L, Rabkin SD, Granato A, Boudah A, Ohara PT (2003) Analgesia and hyperalgesia from GABA-mediated modulation of the cerebral cortex. Nature 424:316-320.

Jasmin L, Granato A, Ohara PT (2004) Rostral agranular insular cortex and pain areas of the central nervous system: A tract-tracing study in the rat. J Comp Neurol 468:425-440.

Kieffer BL, Gavériaux-Ruff C (2002) Exploring the opioid system by gene knockout. Prog Neurobiol 66:285-306.

Kobayashi M (2011) Macroscopic connection of rat insular cortex: anatomical bases underlying its physiological functions. Int Rev Neurobiol 97:285-303.

Kobayashi M, Takei H, Yamamoto K, Hatanaka H, Koshikawa N (2012) Kinetics of $GABA_B$ autoreceptor-mediated suppression of GABA release in rat insular cortex. J Neurophysiol 107:1431-1442.

Koyanagi Y, Yamamoto K, Oi Y, Koshikawa N, Kobayashi M (2010) Presynaptic interneuron subtype- and age-dependent modulation of GABAergic synaptic transmission by β-adrenoceptors in rat insular cortex. J Neurophysiol 103:2876-2888.

Koyanagi Y, Oi Y, Yamamoto K, Koshikawa N, Kobayashi M (2014) Fast-spiking cell to pyramidal cell connections are the most sensitive to propofol-induced facilitation of GABAergic currents in rat insular cortex. Anesthesiology 121: 68-78.

Krettek JE, Price JL (1977) Projections from the amygdaloid complex to the cerebral cortex and thalamus in the rat and cat. J Comp Neurol 172:687-722.

Kuroda R, Kawabata A, Kawao N, Umeda W, Takemura M, Shigenaga Y (2000) Somatosensory cortex stimulation-evoked analgesia in rats: potentiation by NO synthase inhibition. Life Sci 66:PL271-276.

Kuroda R, Kawao N, Yoshimura H, Umeda W, Takemura M, Shigenaga Y, Kawabata A (2001) Secondary somatosensory cortex stimulation facilitates the antinociceptive effect of the NO synthase inhibitor through suppression of spinal nociceptive neurons in the rat.

Brain Res 903:110-116.

Li C, Pleil KE, Stamatakis AM, Busan S, Vong L, Lowell BB, Stuber GD, Kash TL (2012) Presynaptic inhibition of gamma-aminobutyric acid release in the bed nucleus of the stria terminalis by kappa opioid receptor signaling. Biol Psychiatry 71:725-732.

Malmierca E, Martin YB, Nuñez A (2012) Inhibitory control of nociceptive responses of trigeminal spinal nucleus cells by somatosensory corticofugal projection in rat. Neuroscience 221:115-124.

Mansour A, Khachaturian H, Lewis ME, Akil H, Watson SJ (1988) Anatomy of CNS opioid receptors. Trends Neurosci 11:308-314.

Mansour A, Fox CA, Akil H, Watson SJ (1995) Opioid-receptor mRNA expression in the rat CNS: anatomical and functional implications. Trends Neurosci 18:22-29.

McDonald J, Lambert DG (2005) Opioid receptors. Continuing Education in Anaesthesia, Critical Care & Pain 5:22-25.

McDonald J, Lambert DG (2013) Opioid mechanisms and opioid drugs. Anaesthesia & Intensive Care Medicine 14:505-509.

Nakamura H, Kato R, Shirakawa T, Koshikawa N, Kobayashi M (2015) Spatiotemporal profiles of dental pulp nociception in rat cerebral cortex: An optical imaging study. J Comp Neurol 523:1162-1174.

Nakamura H, Shirakawa T, Koshikawa N, Kobayashi M (2016) Distinct excitation to pulpal stimuli between somatosensory and insular cortices. J Dent Res in press.

Nakashima M, Uemura M, Yasui K, Ozaki HS, Tabata S, Taen A (2000) An anterograde and retrograde tract-tracing study on the projections from the thalamic gustatory area in the rat: distribution of neurons projecting to the insular cortex and amygdaloid complex. Neurosci Res 36:297-309.

Ostrowsky K, Magnin M, Ryvlin P, Isnard J, Guenot M, Mauguière F (2002) Representation of pain and somatic sensation in the human insula: a study of responses to direct electrical cortical stimulation. Cereb Cortex 12:376-385.

Pradhan AA, Befort K, Nozaki C, Gavériaux-Ruff C, Kieffer BL (2011) The delta opioid receptor: an evolving target for the treatment of brain disorders. Trends Pharmacol Sci 32:581-590.

Rodgers KM, Benison AM, Klein A, Barth DS (2008) Auditory, somatosensory, and multisensory insular cortex in the rat. Cereb Cortex 18:2941-2951.

Sato F, Akhter F, Haque T, Kato T, Takeda R, Nagase Y, Sessle BJ, Yoshida A (2013) Projections from the insular cortex to pain-receptive trigeminal caudal subnucleus (medullary dorsal horn) and other lower brainstem areas in rats. Neuroscience 233:9-27.

Senapati AK, Huntington PJ, Peng YB (2005a) Spinal dorsal horn neuron response to mechanical stimuli is decreased by electrical stimulation of the primary motor cortex. Brain Res 1036:173-179.

Senapati AK, Lagraize SC, Huntington PJ, Wilson HD, Fuchs PN, Peng YB (2005b) Electrical stimulation of the anterior cingulate cortex reduces responses of rat dorsal horn

neurons to mechanical stimuli. J Neurophysiol 94:845-851.

Senapati AK, Huntington PJ, LaGraize SC, Wilson HD, Fuchs PN, Peng YB (2005c) Electrical stimulation of the primary somatosensory cortex inhibits spinal dorsal horn neuron activity. Brain Res 1057:134-140.

Sessle BJ (2006) Mechanisms of oral somatosensory and motor functions and their clinical correlates. J Oral Rehabil 33:243-261.

Shi CJ, Cassell MD (1998) Cortical, thalamic, and amygdaloid connections of the anterior and posterior insular cortices. J Comp Neurol 399:440-468.

Shigenaga Y, Matano S, Kusuyama M, Sakai A (1974) Cortical neurons responding to electrical stimulations of the rat's incisor pulp. Brain Res 67:153-156.

Svingos AL, Cheng PY, Clarke CL, Pickel VM (1995) Ultrastructural localization of delta-opioid receptor and Met^5-enkephalin immunoreactivity in rat insular cortex. Brain Res 700:25-39.

Tanaka E, North RA (1994) Opioid actions on rat anterior cingulate cortex neurons in vitro. J Neurosci 14:1106-1113.

Treede RD, Apkarian AV, Bromm B, Greenspan JD, Lenz FA (2000) Cortical representation of pain: functional characterization of nociceptive areas near the lateral sulcus. Pain 87:113-119.

Uematsu M, Hirai Y, Karube F, Ebihara S, Kato M, Abe K, Obata K, Yoshida S, Hirabayashi M, Yanagawa Y, Kawaguchi Y (2008) Quantitative chemical composition of cortical GABAergic neurons revealed in transgenic venus-expressing rats. Cereb Cortex 18:315-330.

Viisanen H, Pertovaara A (2010) Roles of the rostroventromedial medulla and the spinal 5-HT_{1A} receptor in descending antinociception induced by motor cortex stimulation in the neuropathic rat. Neurosci Lett 476:133-137.

Viisanen H, Ansah OB, Pertovaara A (2012) The role of the dopamine D2 receptor in descending control of pain induced by motor cortex stimulation in the neuropathic rat. Brain Res Bull 89:133-143.

Yamamoto T, Yuyama N, Kato T, Kawamura Y (1984) Gustatory responses of cortical neurons in rats. I. Response characteristics. J Neurophysiol 51:616-635.

Yamamoto T, Matsuo R, Kiyomitsu Y, Kitamura R (1988) Sensory inputs from the oral region to the cerebral cortex in behaving rats: an analysis of unit responses in cortical somatosensory and taste areas during ingestive behavior. J Neurophysiol 60:1303-1321.

Yamamoto K, Koyanagi Y, Koshikawa N, Kobayashi M (2010) Postsynaptic cell type-dependent cholinergic regulation of GABAergic synaptic transmission in rat insular cortex. J Neurophysiol 104:1933-1945.

Yamamoto K, Takei H, Koyanagi Y, Koshikawa N, Kobayashi M (2015) Presynaptic cell type-dependent regulation of GABAergic synaptic transmission by nitric oxide in rat insular cortex. Neuroscience 284:65-77.

Yasui Y, Breder CD, Saper CB, Cechetto DF (1991) Autonomic responses and efferent

pathways from the insular cortex in the rat. J Comp Neurol 303:355-374.
Zheng W (2010) Activation of mu opioid receptor inhibits the excitatory glutamatergic transmission in the anterior cingulate cortex of the rats with peripheral inflammation. Eur J Pharmacol 628:91-95.
Zollner C, Stein C (2007) Opioids. Handb Exp Pharmacol 177:31-63.